Introduction to Astrophysics

Michaelmas Term, 2020: Prof Craig Mackay

Module 7: Active Galactic Nuclei (AGN).

- Types of AGN, early discoveries, quasars, spectral classes, multi-wavelength observations, emission lines, energetics, variability, basic model.
- QSO host galaxies, anomalous redshifts, radio loud galaxies, the Ly-α forest, the broad-line region (BLR), reverberation mapping, jets, superluminal motion.
- The unified model: central black hole, accretion disk, broad and narrow line regions, dusty torus, jets. Key observations to support the unified model.
- Evolution of the QSO population, scenarios for the evolution of individual AGN, black holes in nearby galaxies, the black hole at the centre of our galaxy and of M87.

1

Active Galactic Nuclei (AGN)

- Many galaxies are seen to have very energetic processes occurring at their centres.
- These are called active galactic nuclei (AGN).
- AGN display high luminosities, non-thermal spectra, variability, emission lines and bright point-like images.
- There is still a lot of work to be done to fully understand AGN but basically it seems that the power source is accretion on to a massive central black hole.

- AGNs come in several forms, indicating a rather heterogeneous classification.

- Seyfert Galaxies – mostly spirals
- Radio Galaxies
- QSO's (which includes quasars)
- Blazars or BL Lac's

2

AGN: Early discoveries

- Emission lines were found in the spectrum of NGC 1068 in 1908 by Edward Fath and Hubble found 2 more galaxies in ~1926.
- In the early part of the 20th century, Carl Seyfert identified a subset of nebulae (before these nebulae were known to be galaxies) which had much more ultraviolet flux and a nucleus with a strong emission line spectrum unlike those seen in HII regions. These are now known as Seyfert galaxies.
- In 1962, Martin Ryle and colleagues in the Cavendish laboratory had undertaken a systematic survey of faint radio sources leading to the publication of the third Cambridge radio catalogue (3CR, standing for 3rd Cambridge Revised).
- The poor positional accuracy (within a few minutes) of this catalogue made optical identifications difficult. Although some were identified with stars or with galactic non-thermal sources such a supernova remnants, most were unidentified.
- A great improvement in positional accuracy was obtained by using lunar occultations. These produced the first really accurate positions (but only for objects along the track of the moon) and led to the identification of a small number of radio sources with blue, star-like objects. These were called ***quasars***.

3

Quasars - Discovery

- The radio source 3C273 was identified as a 13th magnitude star-like object (hence it was called a quasi-stellar radio source or ***quasar***).
- The Dutch astronomer Maarten Schmidt took optical spectra of 3C273 and found a strong emission line spectrum with the lines at unexplained wavelengths. Eventually these were identified with the hydrogen Balmer series at a redshift of z = 0.158.
- Apparently it was receding with a velocity of 47,000 km/sec!

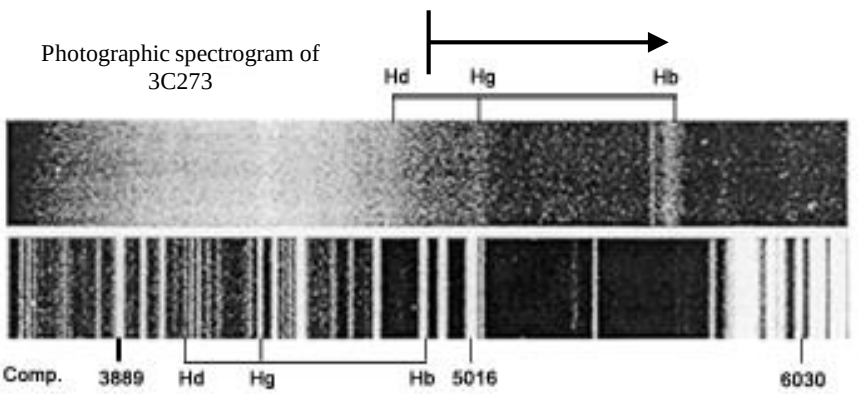

4

Spectrum of 3C273

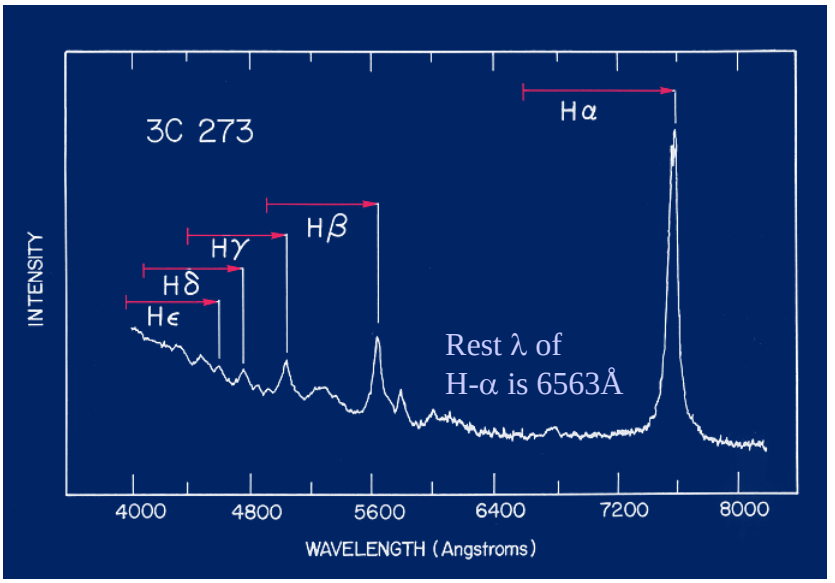

5

Typical (class I) QSO spectrum

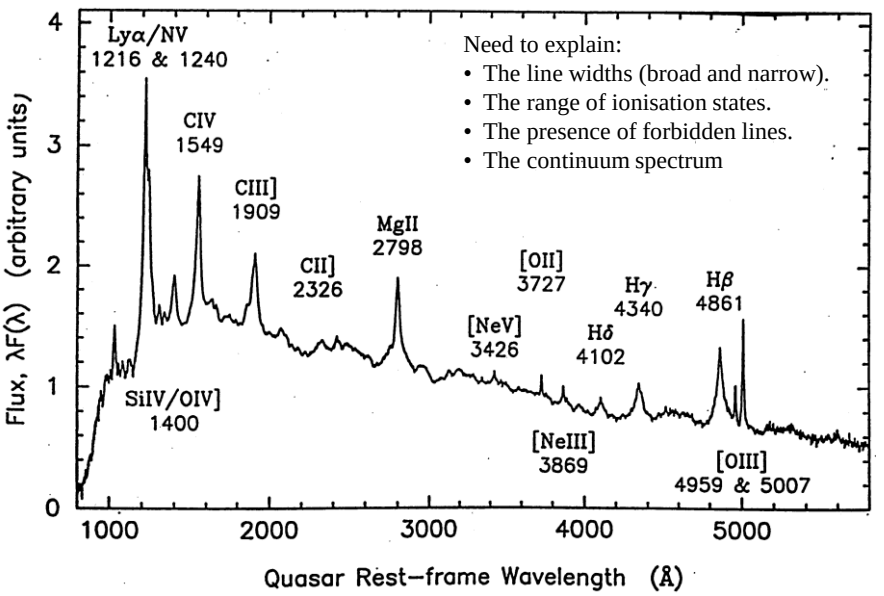

6

Quasars: Discovery

- With ground-based telescopes, quasars are typically boring until you measure their spectrum.
- As a typical example, this is the radio-loud quasar PKS 1117-248 at redshift z=0.466.
- Even at this modest redshift, there is not much of a host galaxy or surrounding group visible to make it stand out.
- This is a red-light CCD image taken with the 3.6-meter telescope of the European Southern Observatory.
- The image covers an area 2.9 by 2.9 arcminutes. The limiting magnitude is about R=23.5.

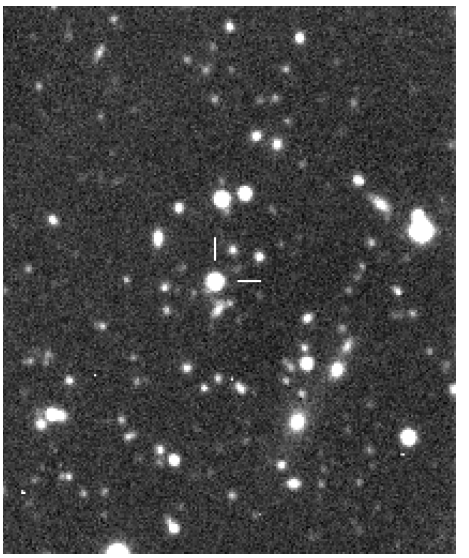

7

Figure from Bill Keel's Web page (Univ Arizona).

QSOs: Discovery

- Their redshift was interpreted as being due to cosmological expansion: this implied that quasars are at very large distances and therefore have very **large luminosities**.
- Soon after the first discovery, objects were detected with redshifts z ~ 2, they had magnitudes in the range m = 13-18, implying that the luminosities were very high, in the range of 10^{39} - 10^{40} W.
- They were also unresolved optically, implying a size < 10kpc.
- A more numerous population of radio-quiet quasar-like objects was discovered. The general term for the whole population (radio-quiet and radio loud) is "***quasi stellar objects***" or ***QSO***s.

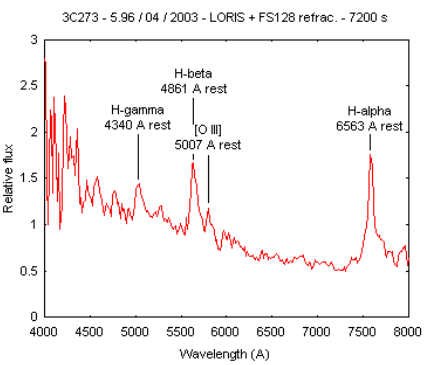

Figure from Bill Keel's Web page (Univ Arizona).

8

QSO colours

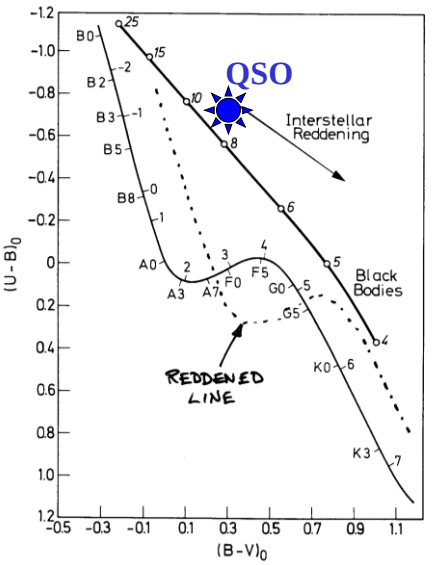

Figure 15.5. Two-color diagram for the main sequence. The reddening-free color indices $(U\text{-}B)_0$ and $(B\text{-}V)_0$ are after H. L. Johnson, W. W. Morgan and others. The MK spectral types and absolute magnitudes of the stars are written along the main sequence. The almost straight line above the main sequence represents black radiators, the numbers are $T_{eff} \times 10^{-3}$ K. Interstellar reddening shifts the position of a star in the diagram parallel to the line in the upper right, which is drawn in particular for O stars.

- Observed QSO colours are very different to observed stellar colours which led to the discovery of many more than were discovered via radio surveys. In fact most QSOs (~90%) are radio-quiet.

9

Classification of Active Galactic Nuclei (AGN)

- QSOs are a specific example of the broader AGN family.
- Classification on the basis of appearance is not very meaningful because the appearance depends on distance and orientation.
- It is better to use a spectroscopic classification scheme which is more related to the intrinsic properties of the AGN.
- Class I: spectra show *broad and narrow emission lines*.
- Class II: spectra show *only narrow emission lines*
- Class III: spectra show *no emission lines* at all but the source has a typical AGN continuum and variability.

Type	Class
Seyfert Galaxies	{I and II}
Radio Galaxies	{I and II}
QSOs	{I}
Blazars (BL Lac's)	{III}

All of these are explained by the ***Unified Theory of AGN*** which we will discuss later.

10

QSOs: Basic Properties: Optical Spectra

- The spectra are characterised by an extended "continuum", and do not have a characteristic black body spectrum.
- There is a lot of short wavelength (high energy) radiation. Because of the high redshifts we can see much more of what is going on in the ultraviolet part of the spectrum.
- The spectrum has prominent emission lines of the common elements such as H, He, C, O, N, S etc.
- The emission lines in the spectra are very broad, typically 5000 - 10000 km s^{-1}.
- The spectra extend over a very wide frequency range, > 15 decades in frequency.
- The spectra may be plotted as functions of wavelength λ or of frequency ν.
- A plot of log (ν) vs log (ν.F(ν)) shows where in frequency space most of the energy is actually emitted. These spectra are of 3C273.

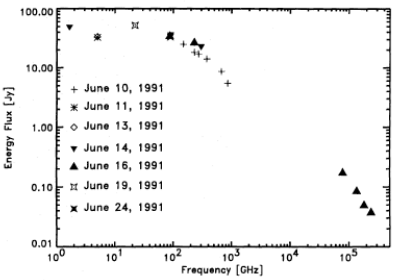

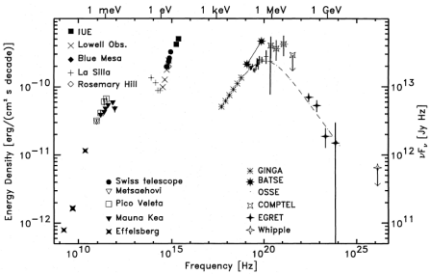

11

Idealised AGN spectral energy distribution

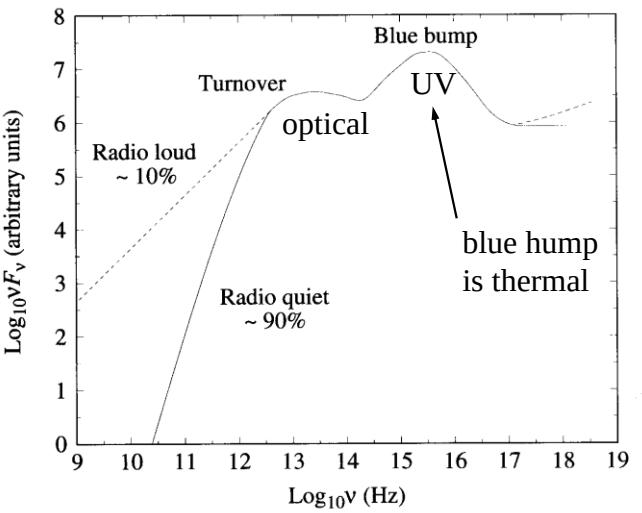

[1] **Figure 26.4** A sketch of the continuum observed for many types of AGNs.

Full spectrum of 3C273

Equal areas under the curve in this plot correspond to equal amounts of energy

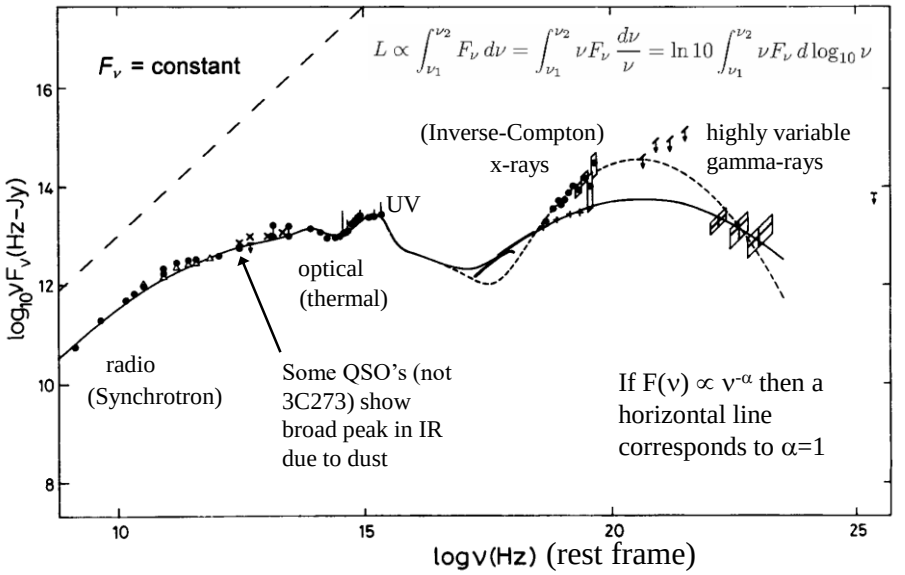

1

QSOs: Basic Properties: Optical Spectra

- It is remarkable that the spectra are close to being flat over many decades in frequency.
- Clearly a QSO is not an object with a blackbody spectrum of a particular temperature. This implies that the we will need non-thermal energy generation to explain the spectral energy distributions of QSOs.
- Synchrotron emission gives us a power law $F(\nu) = \text{constant}. \nu^{-\alpha}$ from an injection of energetic electrons.
- Inverse Compton scattering occurs when relativistic electrons are scattered by low energy photons to a higher frequency.
- We can also make deductions from the broad emission lines in the optical and the ultraviolet:

  If the gas is in thermal equilibrium then from the characteristics of the emission lines ($v \sim 10{,}000$km/s) and using $kT \sim mv^2$, then this implies $T \sim 10^9$ K.
- Because the mass of the carbon atom is ~ 12 times more than that of hydrogen we would expect the width of carbon emission lines to be ~12 times narrower than those of hydrogen if the widths were thermal in origin. However, the widths appear the same.
- Also the Balmer hydrogen lines come from un-ionised gas which cannot exist at $T \sim 10^9$ K. A temperature of $T \sim 10^4$ K is suggested by the ionisation states.
- As a result we conclude that the width of the emission lines must be due to high ***bulk*** velocities rather than a gas temperature of $T \sim 10^9$ K in the emission line regions.

14

AGN: Energetics

- The fluxes and the distances to the quasars imply luminosities L ~ 10^{40} W.
- We can get some information about the lifetimes of AGN from the lobes of radio emission which are on spatial scales ~ 10^5 pc. The lifetime must be greater than the light crossing time so the lifetime > 10^6 years.
- The integrated luminosity over this lifetime suggest an energy E ~ 10^{54} J.
- If this energy was derived from nuclear burning with a 1% efficiency then from $E = Mc^2$, M ~ 1.5×10^8 $M_\odot$.
- This is a minimum requirement with the lifetimes being probably more like 10^7 - 10^8 years and therefore implying an even more extreme luminosity in some quasars.

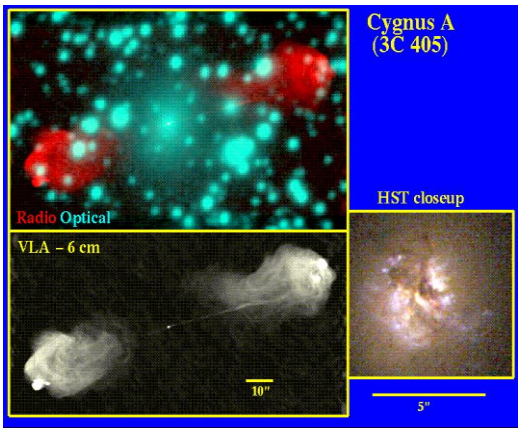

3C405 - An obscured quasar?

- We know that supernovae can inject ~ 10^{44} J into their surroundings. Quasar luminosities would therefore require a supernova event every few hours, fairly improbable from earlier lectures.
- We are forced to conclude that neither nuclear fusion nor supernovae are likely to be viable energy sources for the brightest quasars.

15

(Figure from Bill Keel's Web page (Univ Arizona).)

Cygnus A (3C405)

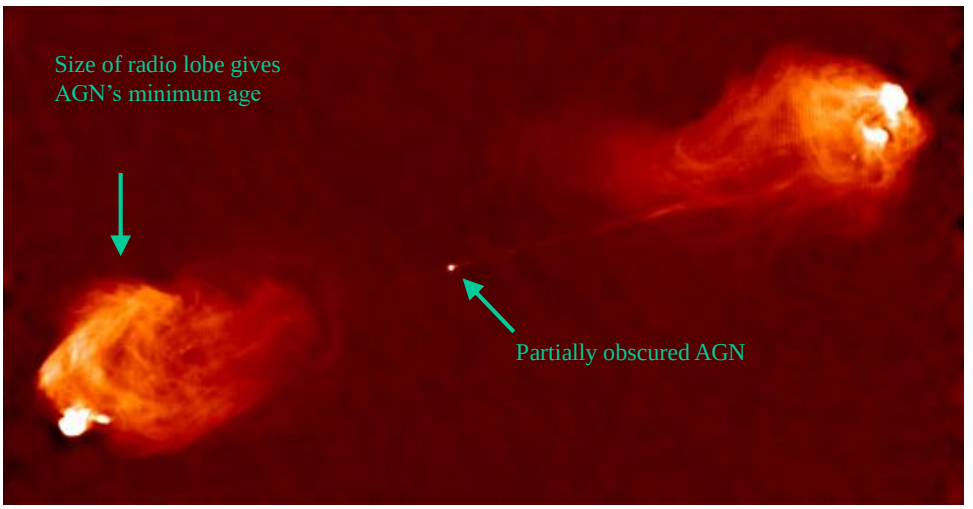

- Although Cygnus A is at a redshift of ~ 0.06 it is the brightest radio source in the sky (after the Sun).
- It is 240 Mpc distant, and about 200 kpc in overall extent. Assumes H ~ 75km/sec/Mpc.

16

AGN are powered by gravitational energy

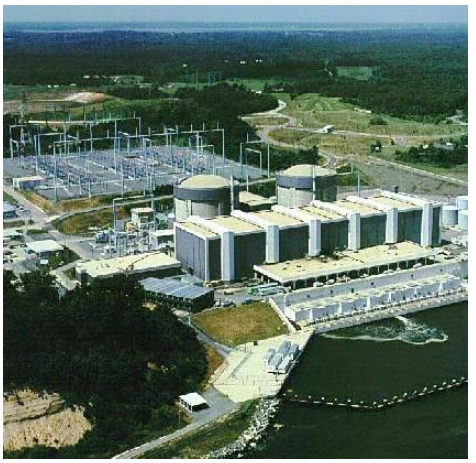

Stars are powered by nuclear reactions

17

Mass accretion rate

We can write

$$\dot{E} = L = \eta \dot{M} c^2$$

where $\dot{M}$ is the mass accretion rate

and η is the efficiency of the process generating the energy (compared to completely converting the rest mass to energy). For black holes calculations show that $0.057 < \eta < 0.423$ with the lower number corresponding to a non-rotating black hole and the upper number corresponding to a maximally rotating black hole. For $L=10^{40}$ W this gives a mass accretion rate in the range:

$$2.6\times10^{23} < \dot{M} < 1.9\times10^{24} \qquad \text{kg/sec}$$

This corresponds to 4-30 solar masses per year.

18

AGN: Variability and the size of the emitting region

- Quasars were discovered to have radio fluxes that varied quite significantly with time.
- We now have access to the full spectral range from radio to gamma-ray wavelengths.
- We find variations in flux by factors of more than two on timescales from months right down to a few hours for the most extreme objects.
- Most Quasars vary slowly if at all.
- The more variable are lower luminosity objects.
- The shortest timescales are observed at the highest energies.
- We will only see a significant flux variation from an emitting region when it size is less than ~ ct, where t is the timescale of variability, though beaming can complicate these ideas.
- This implies the emission regions in quasars are typically smaller than a few light months and in some cases smaller than only a few light days.
- However the luminosities that we are dealing with are between 100 and 1,000 times the luminosity of our galaxy, and all from a region which is approximately the size of the solar system, ~ 10^{14} m.

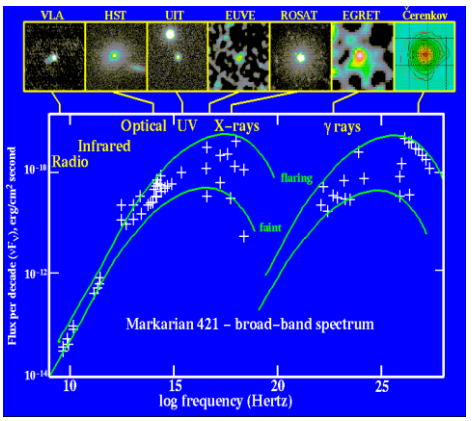

- Markarian 421 (above) is a quasar-like galaxy which shows a substantial variability at virtually every wavelength. The two curves show the limits of the fluxes at different times (x10 variability), and all have the same shape.

(Figure from Bill Keel's Web page (Univ Arizona).)

19

The mass of the emitting region

- For any spherically symmetric region in equilibrium the luminosity must be less than the Eddington luminosity L_{edd} which we saw earlier is given by:

$$L_{edd} \approx 1.5\times10^{31}\frac{M}{M_{sun}} \quad \text{W}$$

- for L=10^{40} W we have M~10^9 M_{sun}. Such a large mass in a small space is clear evidence for a black hole.
- The Schwarzchild radius (which corresponds to the radius of the event horizon for a non-spinning black hole) is given by

$$R = \frac{2GM}{c^2}$$

- for R=7 A.U. (from the variability) we get M ~ 4×10^8 M_{sun}
- Using the virial theorem and the observed line widths we get M ~ 10^9 $M_{sun.}$

20

QSOs: The Basic Standard Model

- The mechanism for generating the necessary energy is accretion of material by a super massive (10^6 - 10^9 M) black hole.
- A model based on this satisfies all the major constraints.
- The efficiency of accretion means that the luminosity can be achieved without very large masses of fuel.
- The black hole mass is consistent with the observed line widths, variability and luminosity.
- The accreting material will reach very high effective temperatures allowing the generation of the observed high-energy photons.
- The accretion disc exists because of the non-zero angular momentum of the accreting material. It is the accretion disk, particularly in the inner region, that is responsible for much of the energy release (as we saw earlier for binary stars).
- The basic model we have, therefore, is of a ***black hole*** with an ***accretion disk***, surrounded by gas that acts as the ***fuel supply***.

21

QSOs: Host Galaxy Properties

- Some astronomers originally suggested that the extreme luminosities of quasars were wrong: i.e. their distances had been overestimated because the redshifts were not cosmological in origin.
- Subsequent studies however show that quasars are indeed at the centre of essentially normal galaxies.
- Initially, detecting the host galaxies was technically difficult. They are much fainter than the QSO which has a luminosity hundreds of times that of a typical galaxy.
- The quasar light is blurred by the atmosphere ("seeing") so that the observed profile of the quasar can swamp the underlying host galaxy.
- The Hubble Space Telescope has provided greatly improved resolution. Nevertheless the low surface brightness of the host galaxies, compounded by the $(1+z)^4$ surface brightness dimming makes the observations difficult, even for the Space Telescope.

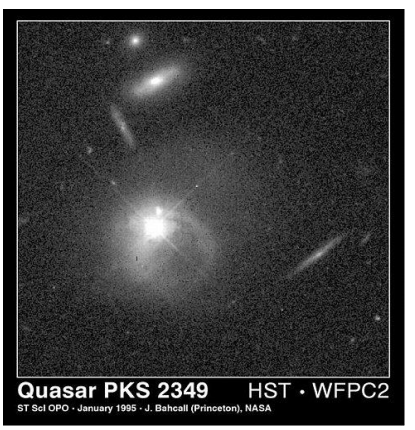

- In this Hubble Space Telescope observation the bright quasar can be seen clearly while the host galaxy is very faint but still quite obvious.

22

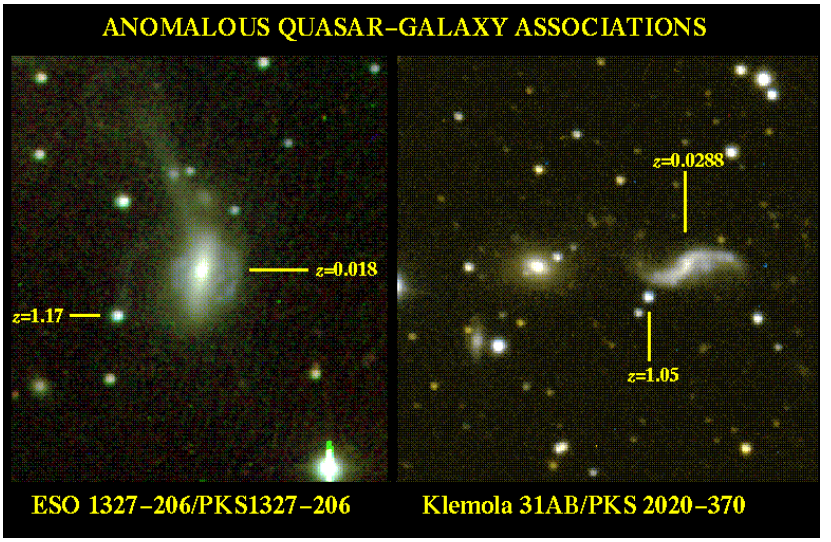

- These problems were not helped because there were a number of apparent associations between high redshifts quasars and low redshifts galaxies.

23

(Figure from Bill Keel's Web page (Univ Arizona).)

Quasars: Host Galaxy Properties

- These spectra show that by careful subtraction of the nuclear light from the QSO it is possible to detect the underlying spectrum of the host galaxy at the same redshift as the QSO.
- These observations strongly support the hypothesis that high luminosity quasars reside within galaxies.

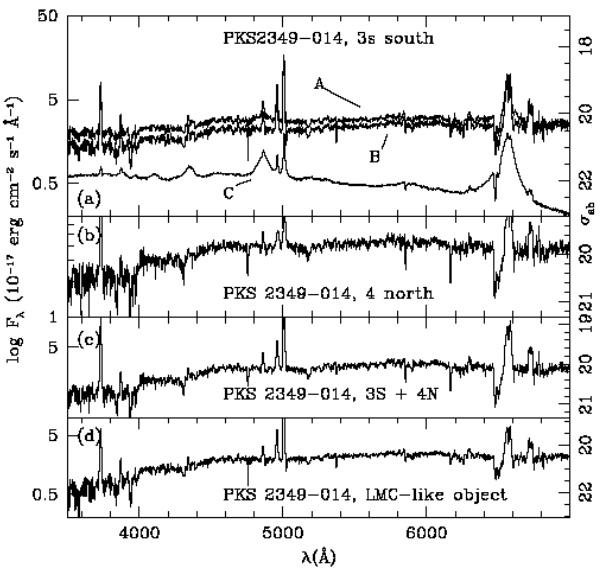

24

FIG. 1.— Four spectra of PKS2349-014: top frame (a) shows the spectra of PKS2349-014 taken at 3 arcseconds south of the nucleus: top curve (A) is the extracted spectrum, middle curve (B) is the residual host galaxy spectrum all position angles co-added, with scattered light subtracted and the bottom curve (C) is the subtracted scatter model ; second frame (b) is the residual host galaxy spectrum taken at 4 arcseconds north of the nucleus; third frame (c) is the co-added spectra from 3 arcseconds south and 4 arcseconds north; bottom frame (d) is the spectrum from the "LMC-like" companion to PKS2349-014. The increased noise at the red end is due to strong OH night-sky lines.

QSOs: Host Galaxy Properties

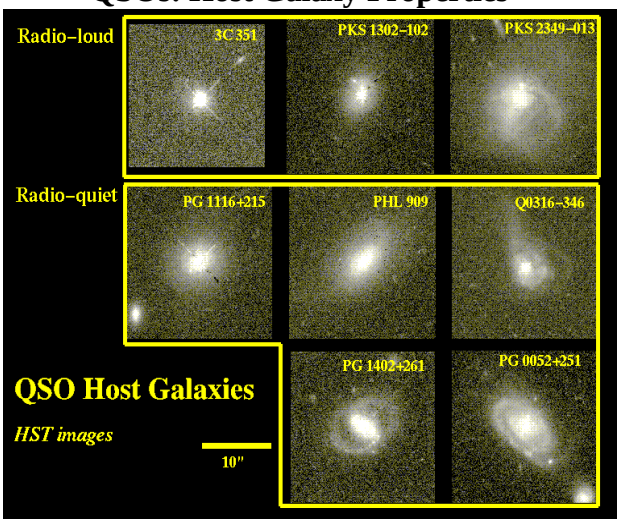

(Figure from Bill Keel's Web page (Univ Arizona).)

- One idea that had been considered attractive is that the difference between "radio-loud" and "radio-quiet" quasars might be due to their different location in different types of host galaxy.
- This would suggest that the development of radio structure depends on the environment of the galaxy.
- More recent work, however, does not support this scheme. (McLure et al, MNRAS, 308, 377, 1999)

25

The Lyman-alpha forest in a QSO spectrum

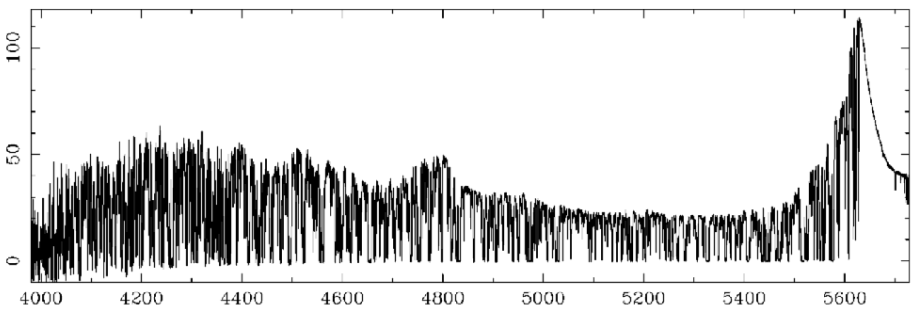

Figure 1 High resolution [full width at half maximum (FWHM) $\approx$ 6.6 km s^{-1}] spectrum of the z_{em} = 3.62 QSO1422+23 (V = 16.5), taken with the Keck High Resolution Spectrograph (HIRES) (signal-to-noise ratio ~150 per resolution element, exposure time 25,000 s). Data from Womble et al (1996).

The absorption lines blueward of the Ly-alpha emission line are due to clouds of hydrogen along the line of sight

26

The Lyman-alpha forest in a QSO spectrum

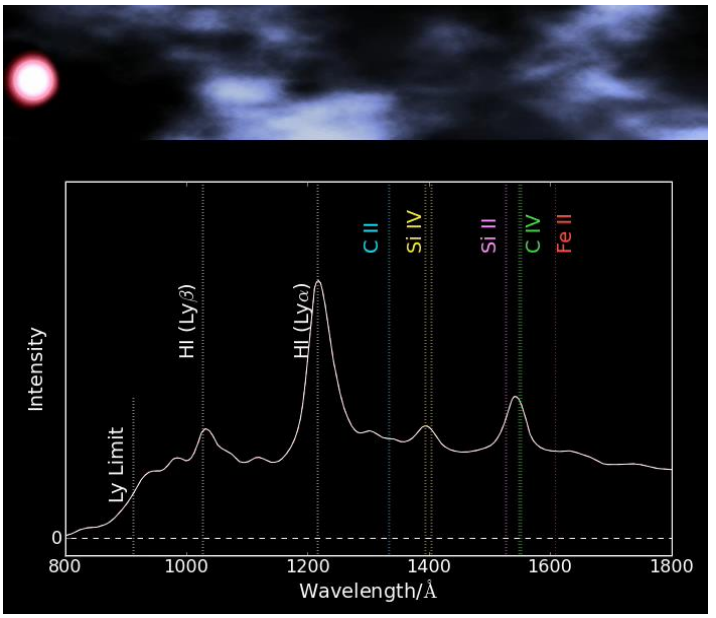

27

Quasars: Basic Properties: Broad Line Region (BLR)

- The Broad Line Region (BLR) is the gaseous region where the QSO's broad spectral emission lines originate.
- In this region the velocity widths of the emission lines are approximately constant. As we have already seen this rules out the explanation that the gas is in thermal equilibrium because kt is very different from mv^2.
- The explanation for the large velocity widths (5,000-10,000 kilometres per second) is high velocity bulk motions (high velocity clouds).
- Quasar spectra clearly show features from low-ionisation species implying that the temperature of the gas clouds must be in the region of 10,000 K.
- Can we estimate the density of the gas within the broad line region?
- If we imagine that the gas of the broad line region is irradiated by photons from the accretion disk we can see that the excitation of the gas may be by photo ionisation and recombination as well as by collisional excitation.
- The de-excitation processes will be by radiation (which we see as emission lines in the spectum) as well as by collisional de-excitation.

28

Quasars: Basic Properties: Broad Line Region (BLR)

- The lifetime of an ion with an electron in an excited state is determined by its "Einstein coefficient". For example, A_{21} for transitions from level 2 to level 1.
- Quantum mechanical rules determine whether a particular transition is likely (for a permitted transition) or unlikely (for a forbidden transition).

  A permitted transition: $A_{21} \sim 10^8\ s^{-1}$.

  A forbidden transition: $A_{21} \sim 10^2\ s^{-1}$.
- The lifetime of an ion in a particular state is then ~ 1/A.
- If an ion in an excited state encounters another particle within a time t ~ 1/A then a collisional de-excitation will occur.
- In the case of forbidden transitions, a collisional de-excitation causes the ion to return to a lower energy state so a photon is not emitted and the transition is not seen.
- Therefore, for forbidden (or semi-forbidden) transitions, as the density of particles increases and the frequency of collisions increases, the probability of the transition occurring drops. This causes a reduction in the line emission from that transition.
- Once the mean time between collisions is $< 1/A_{21}$, the forbidden transition is no longer seen.
- This is essentially a critical density for that emission line.

29

Quasars: Density Estimate for the Broad Line Region

- The mean time between collisions is proportional to the inverse of the density of the gas.
- By looking for the emission from forbidden or semi-forbidden transitions we can calculate the density.
- We start by assuming a temperature for the gas, say, 10^4 K. If we take then, for example, the semi-forbidden emission line from CIII] at 190.9 nm we can compare its strength with other similar species such as CIV or even with Lyα. This lets us plot the emission line intensity ratios such as Lyα/CIV and CIII]/CIV.
- By looking at the ratios of emission line intensities we can reduce the uncertainty there would otherwise be in the relative abundances of the different species.
- We find that, as the density rises, the ratio of Lyα/CIV is little affected whereas the ratio of CIII]/CIV changes only slightly until a critical density of ~ $10^{16}\ m^{-3}$ is reached.
- We conclude, therefore that if the CIII] 190.9nm line is present in the quasar spectrum then the density $n < 10^{16}\ m^{-3}$.

30

Quasars: Size Constraints for the Broad Line Region

- Many quasars show very significant changes in the continuum flux.
- The maximum size of this continuum source must be the velocity of light multiplied by the timescale for change.
- This implies that the continuum source must be very small, in some cases $< 10^{14}$ m.
- The broad line emission region surrounds the continuum source and is illuminated by that source.
- The total flux from the object varies for several reasons including:
  * the number of ionising photons from the accretion disc changes
  * the gas in the broad line region is more or less ionised
  * there are more or fewer excited ions
  * and there are stronger or weaker emission lines.

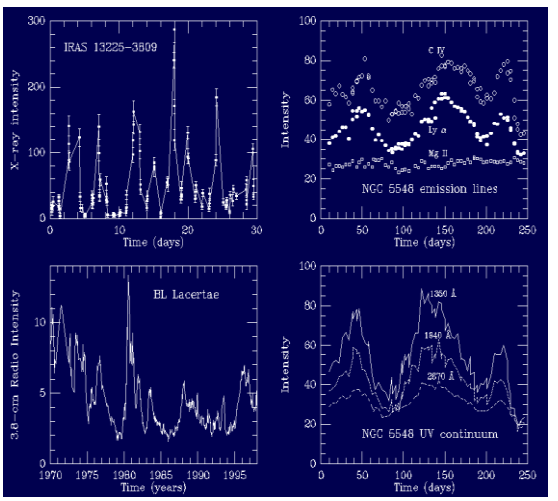

- We can monitor the emission line fluxes following sudden changes to the continuum flux such as those shown in the above picture at different wavelengths.
- By measuring these time delays we can determine the size of the broad line region.
- We must be careful to use emission lines from species where the lifetimes are short and where the response to the changing continuum flux will be rapid.

31

QSOs: The Model So Far

- We can summarised our basic model so far:
- There is a central black hole with mass M ~ 10^7 - 10^8 $M_\odot$.
- Around it is an accretion disc in which the material is expected to have a non-zero angular momentum.
- Accretion onto the disk and mass flow from the outside to the inside of the disc generates large amounts of energy from a volume that is only a few light hours across ~ 10^{13} m.
- Outside this region is the broad line region containing large numbers of clouds which are replenished and maintained by the radiation from the central continuum source which is balanced by the emission of the clouds.
- These clouds have an internal temperature T ~ 10^4K, particle density ~ 10^{16} m^{-3}, velocity dispersion of the clouds v ~ 3000 km s^{-1} and a size of typically ~10^{15} – 10^{16} m (light months).
- Can we do better than this in trying to work out the size of the broad line region and in understanding the kinetics of the clouds within it?

32

QSOs: Reverberation Mapping

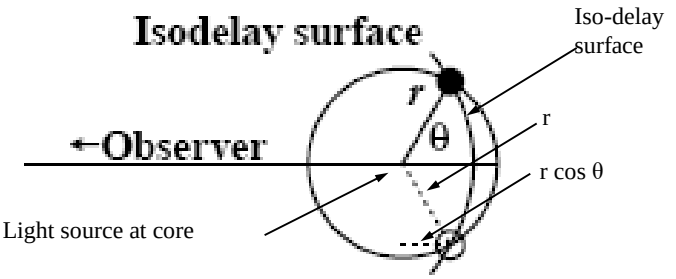

- If there is a sudden change in the continuum luminosity from the core, how does this affect the broad line region?
- If we imagine BLR clouds distributed in a sphere centred on the central continuum source then the emission line clouds will respond to a continuum outburst with an observed time delay of $\tau = (1+\cos\theta)r/c$. The iso-delay surface has τ = constant.
- We can think of the surface from which we will see radiation at a particular time after it left the core as being a parabolic "isodelay surface". Like the optics of a flash light reflector or a telescope in reverse.
- For a spherical shell of radius r, in a broad line region, the intersection with an iso-delay surface is a ring of radius $r.\sin\theta$, and surface area $2\pi(r.\sin\theta).(r.d\theta) = 2\pi r^2 \sin\theta.d\theta$.

33

QSOs: Reverberation mapping

Assume the BLR is spherically symetric and the pulse of light produces a response ε per unit area. The observer will see a contribution from the ring of

$$\psi(\theta)d\theta = 2\pi r^2 \varepsilon \sin\theta.d\theta$$

And the whole emission line response at a given moment will be

$$\Psi = \int \psi(\theta)d\theta$$

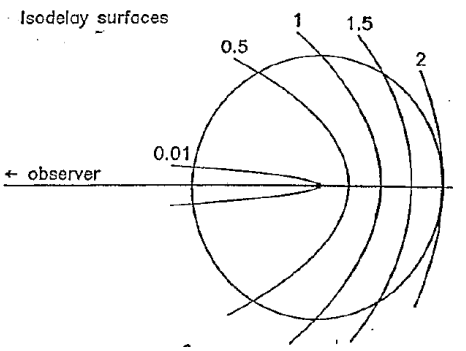

The *average* distance of an iso-delay surface (from the centre of the BLR) increases as τ increases.

FIG. 1—Schematic view of the BLR as a thin spherical shell. The observer, to the left at infinity, sees continuum pulses propagate outward as paraboloids. At any time τ following the detection of the continuum pulse, the observer sees a response from the gas at the intersection of the BLR and an isodelay surface (with the appropriate value of τ labeled in units of r/c, where r is the BLR radius).

34

QSOs: Reverberation mapping

Range of θ corresponding to intervals of time

$$\tau = (1+\cos\theta)\frac{r}{c} \quad \Rightarrow \quad \frac{d\tau}{d\theta} = -\frac{r}{c}\sin\theta$$

$$\Rightarrow \quad \psi(\tau)d\tau = \psi(\theta)\left|\frac{d\theta}{d\tau}\right|d\tau = 2\pi.\varepsilon.r.c.d\tau$$

Thus the contribution of a spherical shell to the change in an emission line is constant from

$$\tau = 0 \quad (\theta = 180^\circ) \quad \text{to} \quad \tau = \frac{2r}{c} \quad (\theta = 0^\circ)$$

35

Quasars: Reverberation Mapping

- We can observe the time behaviour of different emission lines and compare it to the variation seen in the continuum flux.
- In the galaxy shown here that the longest delays are seen for the emission lines which have the lowest ionisation potential.
- This implies that species with higher ionisation potentials are closer to the continuum source.
- We also find, when we compare different galaxies with one another, that the time lags are proportional to the luminosity of the source implying that the more luminous quasars possess larger broad line regions.
- The origin of the clouds is unclear. The mass in the clouds is tiny, ~ 10^{-5} $M_\odot$.
- One model identifies the clouds as being the ionised outer atmospheres of stars.

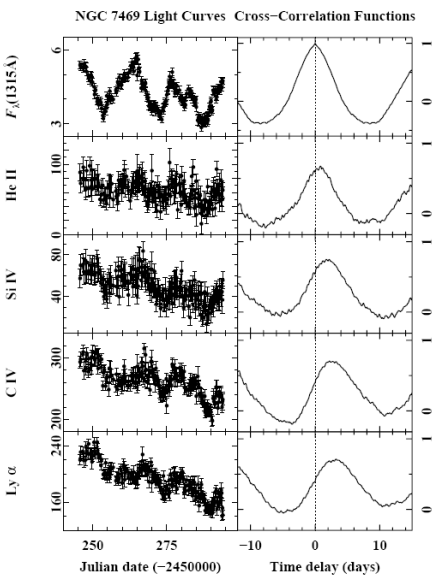

36

QSOs: Reverberation mapping, Internal motions

- At a given moment in time an observed spectral line comes from the whole iso-delay surface.
- If we break the emission line up into several wavelength bins we are looking at clouds with different line of sight velocities.
- Each of these will come from different parts of the iso-delay surface.
- In principle, the data could be analysed to put constraints on how the BLR clouds are moving around: infalling, outflowing, orbiting or moving randomly.
- Velocities determined in this way can then be used to put constraints on the black hole mass. Similar to when we worked out the BH mass using the virial theorem but not relying on the BLR actually being in virial equilibrium (which it almost certainly isn't).

37

AGN: Jets and Beamed Radiation

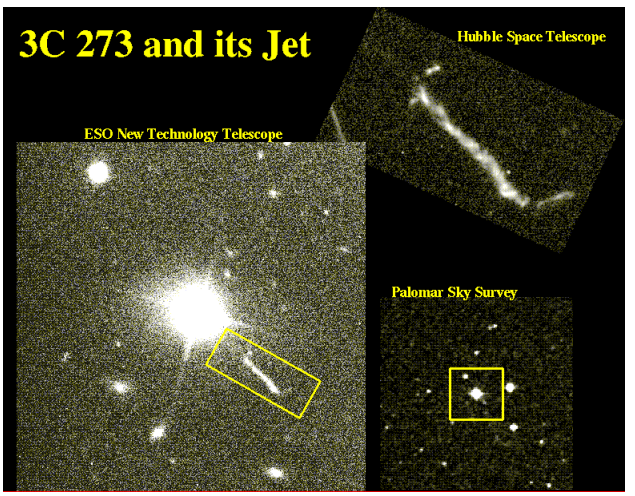

(Figure from Bill Keel's Web page (Univ Arizona).)

- The first quasar discovered was 3C273 and it shows a clear optical jet which is visible at many wavelengths (see picture above).
- To understand the jets we see in AGN we need to consider many details including the energetics of the jet, how they are collimated and what their dynamics might be.

38

AGN: Jets and Beamed Radiation

- Over the years there have been many improvements in technology. Photography has given way to the use of charge coupled devices (CCD) on telescopes, including the Hubble Space Telescope.
- This beautiful picture shows the jet in M87 as being much bluer than the background galaxy.
- M87 is as supergiant elliptical galaxy at the centre of the Virgo cluster.
- It is a strong radio source with emission both from the nucleus and particularly from the jet.
- The many spots on this picture are faint globular clusters.
- There is a population of about 15,000 globular clusters in this galaxy.
- This jet has many of the properties of QSO jets.

39

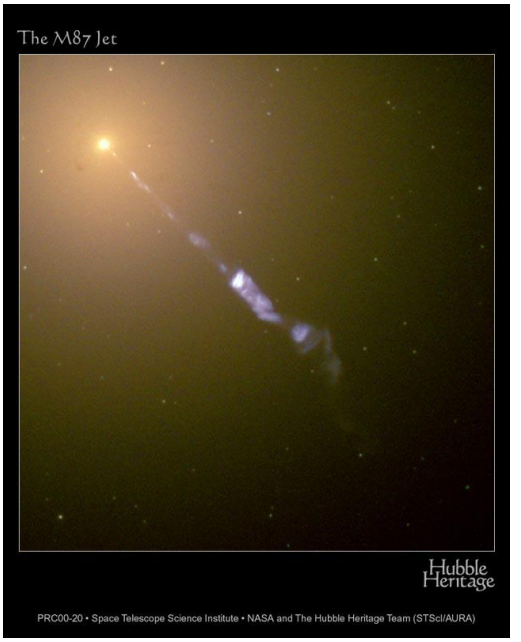

AGN: The Black Hole in M87

- Recently astronomers have combined large area radio telescopes across the whole world.
- M87 is a strong radio emitter with a lot of flux from its central core.
- The calculations we have just done make it most likely that the centre of this galaxy hosts a blackhole and that much of the emission must come from the accretion disc around it.
- By combining radio signals from many different observatories, astronomers were able to produce an image at radio wavelengths of the very centre of this galaxy.
- The data has been used now by the Event Horizon Telescope (EHT) collaboration to construct the movie at 1.3mm wavelength.
- Ring is 42 μarcsecs in diameter.
- Consistent with $6.5 \times 10^9 M_\odot$ Black hole.

40

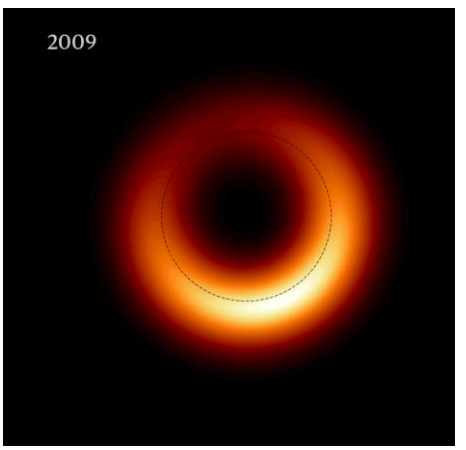

AGN: Jets and Beamed Radiation

- Advances in radio telescope technology have allowed Very Long Baseline Interferometry (VLBI) to achieve astonishing angular resolution.
- This allows us to track the motions of the components of jets.
- We see *apparent* motion several times faster than the speed of light.
- This is known as superluminal motion.
- Like 3C273 which we saw earlier, 3C279 is a superluminal radio source.

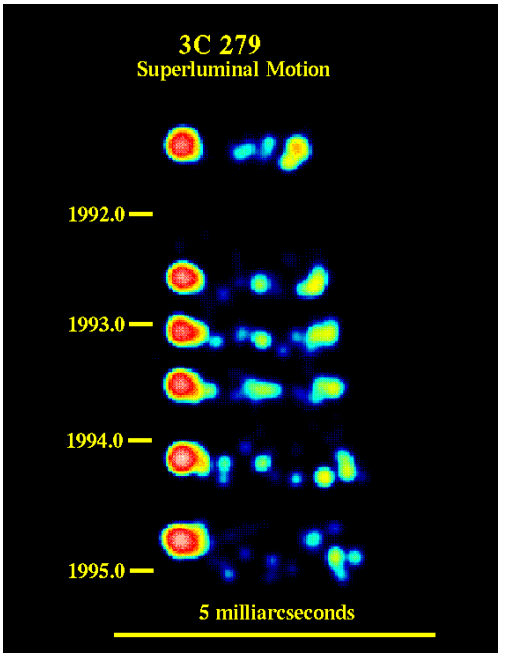

(Figure from Bill Keel's Web page (Univ Arizona).)

41

AGN jets: Superluminal Motion

- We see the same sort of activity in the jet in the giant elliptical galaxy M87.
- There are many examples of this superluminal phenomenon.
- This shows just a very small part of the jet closest to the nucleus of the giant elliptical galaxy. Marked on the diagram are the fronts corresponding to different blobs that have been identified and tracked together with their *apparent* superluminal velocities.

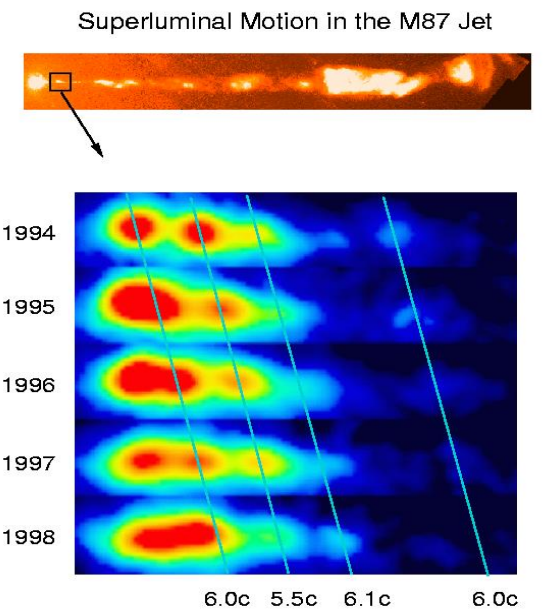

(Figure from Bill Keel's Web page (Univ Arizona).)

42

AGN jets: Superluminal Motion

- According to the theory of relativity things cannot move faster than the speed of light. So how do we explain superluminal motion?
- The observer views a hotspot in the quasar jet at one position and one time, and then later views the same apparent hotspot at a new position and time having moved a distance $v.t_e$.

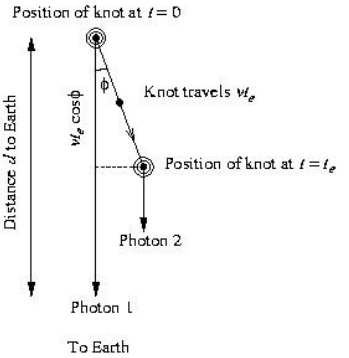

- The first photon reaches earth at a time t_1:

$$t_1 = \frac{d}{c}$$

- the second photon at time t_2:

$$t_2 = t_e + \frac{d - \mathrm{v}t_e \cos\phi}{c}$$

- the time interval between these two photons being received on Earth is Δt:

$$\Delta t = t_2 - t_1 = t_e\left(1 - \frac{\mathrm{v}}{c}\cos\phi\right)$$

43

AGN jets: Superluminal Motion

- The apparent transverse velocity measured is given by [1]:
- solving for v/c we get [2]:
- Given that we know v/c < 1 this constrains the angle φ: (to get lower limit, set v/c=1 and solve for cos φ, upper limit is obvious)
- and the smallest possible v/c is then given by [4] (differentiate [2] and set to zero).
- v_{min} corresponds to an angle φ_{min}
- this minimum v/c gives the minimum Lorentz factor of the source of:
- from this we see that apparent transverse velocities > c are possible. In fact transverse velocities observed to be > 10c are not uncommon.

$$\mathrm{v}_{\mathrm{app}} = \frac{\mathrm{v}t_e \sin\phi}{\Delta t} = \frac{\mathrm{v}\sin\phi}{1 - \frac{\mathrm{v}}{c}\cos\phi} \qquad [1]$$

$$\frac{\mathrm{v}}{c} = \frac{\mathrm{v}_{\mathrm{app}}/c}{\sin\phi + (\mathrm{v}_{\mathrm{app}}/c)\cos\phi} \qquad [2]$$

$$\frac{\mathrm{v}_{\mathrm{app}}{}^2/c^2 - 1}{\mathrm{v}_{\mathrm{app}}{}^2/c^2 + 1} < \cos\phi < 1 \qquad [3]$$

$$\frac{\mathrm{v}_{\mathrm{min}}}{c} = \sqrt{\frac{\mathrm{v}_{\mathrm{app}}{}^2/c^2}{1 + \mathrm{v}_{\mathrm{app}}{}^2/c^2}} \qquad [4]$$

$$\cot\phi_{\mathrm{min}} = \mathrm{v}_{\mathrm{app}}/c$$

$$\gamma_{\mathrm{min}} = \frac{1}{\sqrt{1 - \frac{\mathrm{v}_{\mathrm{min}}{}^2}{c^2}}} = \sqrt{1 + \frac{\mathrm{v}_{\mathrm{app}}{}^2}{c^2}} = \frac{1}{\sin\phi_{\mathrm{min}}}$$

44

AGN: The Unified Model

- So far we have a rotating central massive black hole (10^6-10^9 $M_\odot$).
- Material falling in to the very deep potential well (1-10 $M_\odot$ yr^{-1}).
- A rotationally aligned accretion disk (radiation is created here).
- A region filled with high velocity clouds of gas (the broad line region - BLR) which surrounds the central black hole.
- Extremely high velocity jets.
- Still need to explain:
  - The narrow spectral emission lines
  - The various spectral classes
- We can add a torus of surrounding dust and gas and an outer region of low velocity clouds (the narrow line region - NLR).
- This gives us the ***unified model for AGN*** which is a single model that explains most of the observed features of AGN.

45

The Unified Model: AGN spectral classes

- QSOs, quasars, Seyfert 1 galaxies, broad line radio galaxies, and N-galaxies have **broad and narrow emission lines** in their spectra and are known as ***Class-I*** objects.
- In addition Seyfert 2 galaxies, narrow line radio galaxies and "liners"* **only have narrow emission lines** in their spectra and are known as ***Class-II*** objects.
- ***Class-III*** objects includes blazars, BL Lac objects and optically violently variable quasars (OVVS). These have **no emission lines** in their spectra.

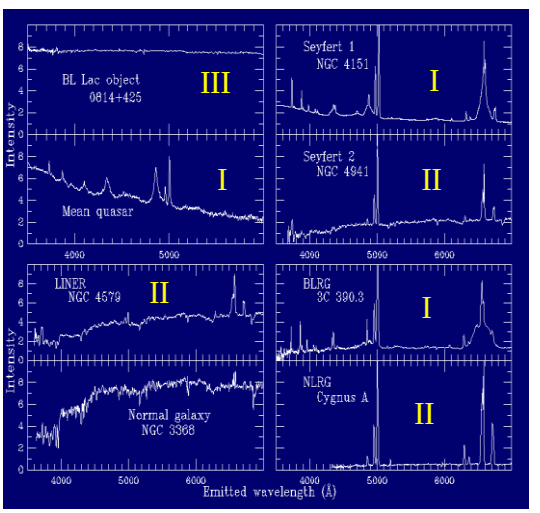

* LINER = Low Ionisation Nuclear Emission-line Region

46

The AGN unified model

The broad line region is clumpy and close to the centre. Clouds fill ~1% of the volume. Variability of the broad lines indicates a size of ~10^{16} metres (~1pc).

Various classes are due to the viewing angle.

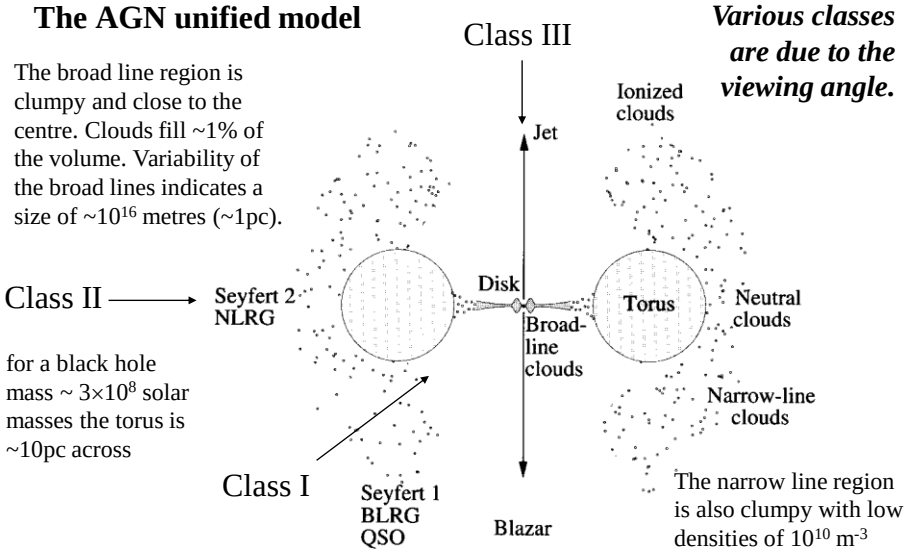

Figure 26.25 A sketch of a unified model of an active galactic nucleus. The jets would be present in a radio-loud AGN. A typical observer's point of view is indicated for AGNs of various types.

47

The AGN Unified Model

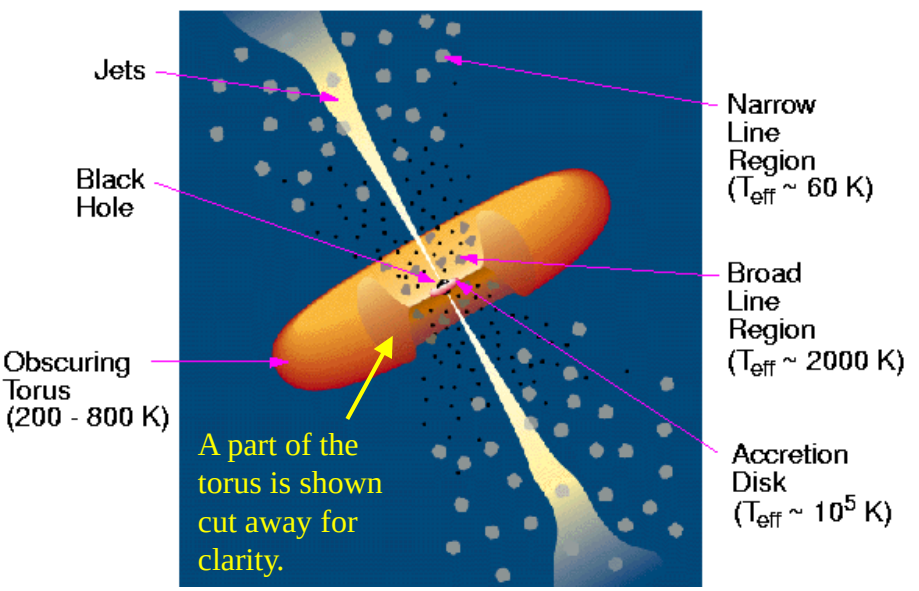

48

A detailed model of an AGN accretion disk

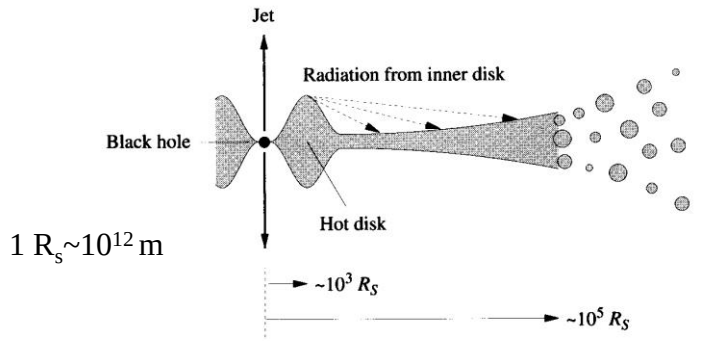

Figure 26.23 A possible structure of the accretion disk in an AGN.

- In the inner region of the disk, out to about 1000 R_S, the radiation pressure dominates giving a thick hot disk. This produces the blue bump in the spectrum.
- Further out (to about 10^5 R_S) is a thin disk supported by gas pressure. The surface of this is illuminated by the hot disk possibly giving rise to winds.
- Beyond 10^5 R_S the disk breaks up in to numerous clouds.

49

The Unified Model for AGN: The accretion disk

- We can achieve a good match to the observed spectral energy distribution of QSOs at ultraviolet and soft x-ray wavelengths by assuming the material at radius r in the disk radiates as a black body with temperature T, where T increases with decreasing radius r (see earlier lectures on accretion disks for binary stars).

- Integrating the black body spectrum at each radius and summing the components to give the spectral energy distribution from the whole disk produces a broad peak in the spectral energy distribution at ultraviolet wavelengths, with an equivalent black body temperature T ~ 100,000 K.

50

The Unified Model for AGN: The BLR

- In the broad line region (BLR) the high energy photons from the accretion disk ionise the gas in the high velocity clouds.
- The ions then recapture electrons and emission lines are produced as the electrons cascade down from high excitation bound states to lower ones.
- The width of the lines is due to the high velocities (~2,000 – 10,000 km/s) of the individual clouds.
- It is not clear whether any significant ordered motion (either outwards due to radiation pressure or inward due to the gravitational attraction of the central object, or rotation) exists in addition to the very high random velocities.

51

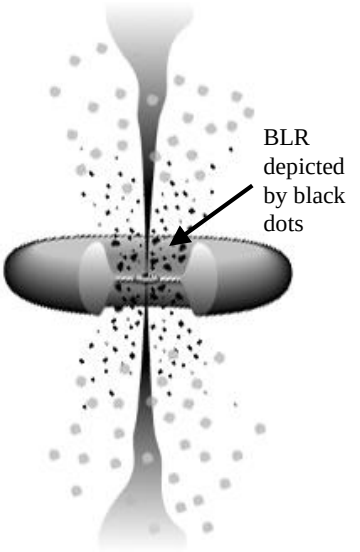

Figure from Rieger, Ph D thesis, Gottingen,2000.

The Unified Model for AGN: The optically thick torus

- The dusty optically thick gas torus is about 10pc across. Radiation from the central source heats the dust in parts of the torus to a temperature between 1000 and 1500 K, producing a maximum in the spectral energy distribution at infrared wavelengths, something that is seen commonly in many quasars and active galactic nuclei.

- The dusty torus also has the effect of producing a weak collimation of the photo ionising radiation, confining the escape of optical , ultraviolet and soft x-ray photons into two cones. The ionisation produced by this radiation occurs away from the equatorial plane of the torus.

52

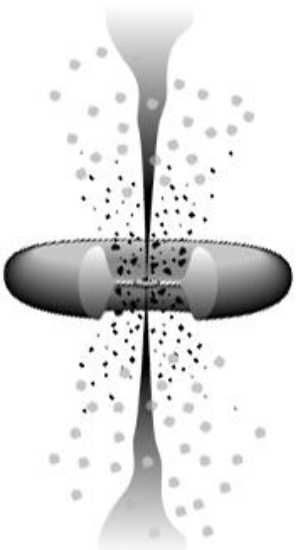

Figure from Rieger, Ph D thesis, Gottingen,2000.

The Unified Models for AGN: Jets

- In approximately 10% of QSOs (those which are radio loud) a highly collimated relativistic beam of electrons emerges from the central object.
- It may be that the collimation of these beams depends on the dynamics of the accretion disk and it may also be the case that the direction is further collimated by the presence of magnetic fields.
- Conservation of momentum implies that it is likely that two beams will propagate in opposing directions and this is what is normally observed.
- One-sided jets are observed in radio sources when the jets are viewed close to the line of sight and a relativistic boosting of the radiation along the line of sight dramatically enhances the radiation received from the approaching jet as well as reducing the radiation received from the receding jet.

53

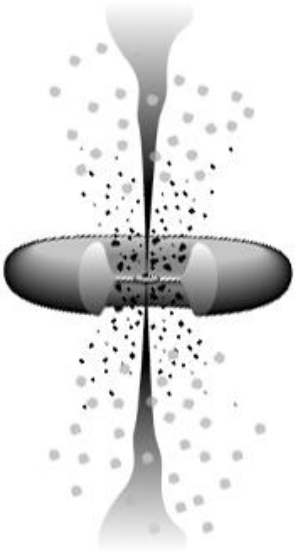

Figure from Rieger, Ph D thesis, Gottingen,2000.

The Unified Model for AGN: Jets

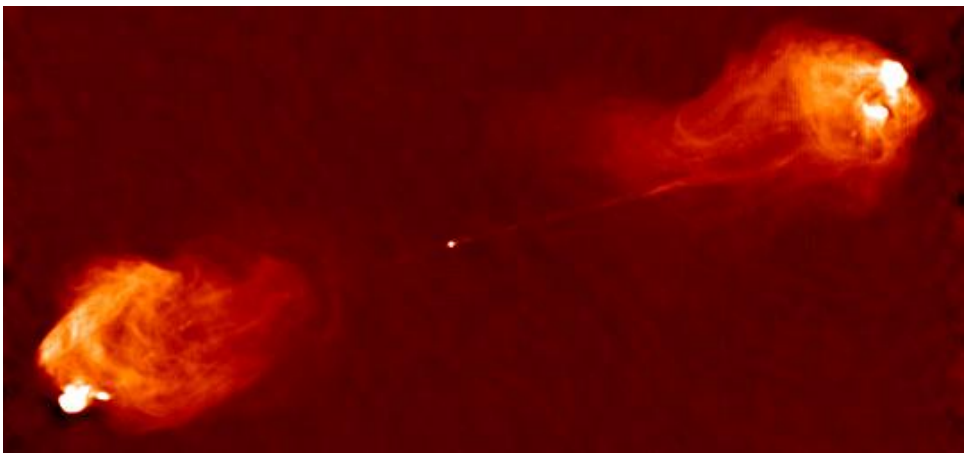

- This image is a radio map of the extremely bright radio galaxy, 3C405 or Cygnus A.
- This is a classic double radio source, with streams of energetic particles shot out in opposite directions, eventually being decelerated in the turbulent boundary with the intergalactic medium.
- All the radiation shown above is synchrotron radiation. This structure is optically invisible.

54

The Unified Model for AGN: Jets

- Unified schemes for radio loud QSOs are particular successful but there is still no full explanation as to why about 10% of all QSOs should possess relativistic jets.
- A popular idea is that the environment surrounding the central source is important and that the different properties of the interstellar medium in elliptical and spiral galaxies are related to the presence or absence in these objects of jets.
- Very broadly speaking, elliptical galaxies tend to host radio loud active galactic nuclei and spiral galaxies tend to host radio quiet objects.
- Note that the rotation axis of the AGN's accretion disk and the rotation axis of the host galaxy's spiral arms are not necessarily aligned.

55

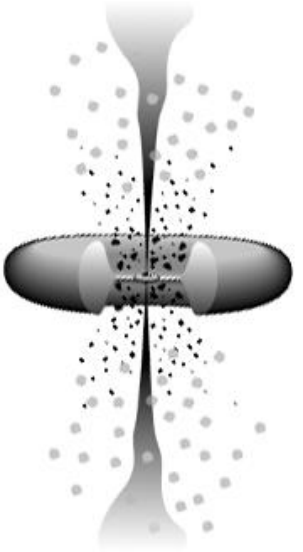

Figure from Rieger, Ph D thesis, Gottingen,2000.

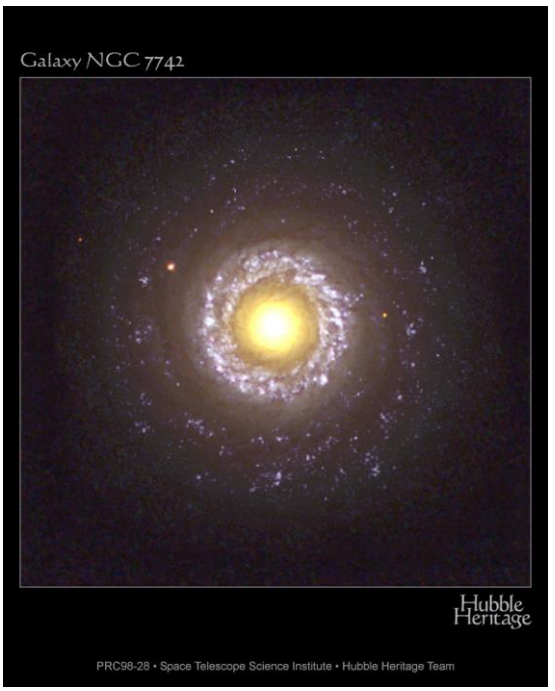

56

NGC 7742 (Seyfert-2)

The spiral disk and the accretion disk are not aligned.

The Unified Model for AGN: Further Observational Evidence

- The unified model explains many observations including the luminosities, the excitation and ionisation states, the emission lines, the variability, the radio, IR, optical, x-ray and gamma ray emission, etc.
- Four further things can be seen which support the unified model.

1. In class III AGN the BLR and NLR can be seen when the spectra have high enough signal-to-noise to overcome the dazzling effect of looking straight down the jet.
2. The dusty torus in NGC1068 may have been seen directly by radio telescopes.
3. In class II AGN the BLR can be seen via scattered (polarised) light.
4. There is a good correlation between the luminosity in the continuum and the luminosity of the emission lines for a very wide range of AGN types supporting the idea that they can be explained by a single model.

CCD image of the Seyfert-2 spiral galaxy NGC1068, a galaxy with a faint outer ring. This digital photograph , taken with the MIT/Lincoln Labs CCD camera on the 3.9-meter Anglo-Australian Telescope, shows detail over a wide dynamic range, including the bright starburst inner disk and star-forming regions in the outer arms.

57

Seeing the central regions of a type-II AGN

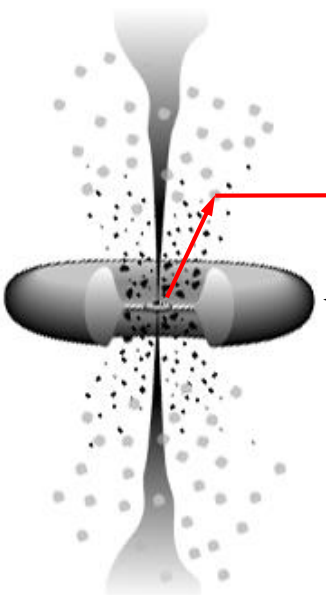

Scattered (polarised) light from the accretion disk and the BLR gets to us on Earth.

Our view from Earth of the accretion disk and the BLR is blocked by the torus which is optically thick.

58

The Unified Model for AGN: Spectropolarimetry

- Scattering or incoherent reflection produces polarised light – just like reflections off a swimming pool.
- In NGC 1068, a combination of polarimetry and spectroscopy show the *unpolarised* spectrum is Type 2 with virtually no Fe II and much narrower hydrogen lines.
- the *polarized light* from the nucleus resembles a Type 1 Seyfert, with broad Balmer lines of hydrogen and forests of blended Fe II emission at 450 and 530 nm.
- This implies that the polarized light comes from dusty clouds that are situated directly in the radiation field of the nucleus, so that we see the nuclear light scattered by dust.

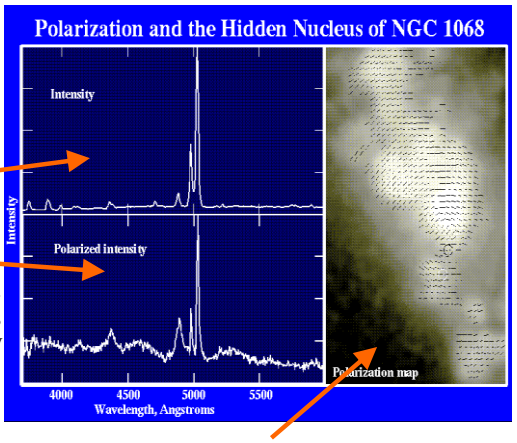

- A striking confirmation that the nucleus is responsible comes from an HST measurement of the polarization at every point near the nucleus.
- These are shown as electric-field direction vectors superimposed on the image.
- They show the characteristic pattern of concentric arcs which results from scattering by a source in the centre, and points to the same centre as the radio jets and tracing backwards from the conical distribution of ionized gas around the nucleus.

59

(Figure from Bill Keel's Web page (Univ Arizona).)

The Unified Model for AGN: Directly imaging the torus?

- In NGC 1068 the nucleus produces a radio jet at right angles to the hypothesized torus, which must lie almost at right angles to the galaxy's disk plane.
- Very Long Baseline Interferometry (VLBI) radio observations may have detected this torus, as shown in this montage.
- The first HST image shows the galaxy as a whole.
- The second HST image shows the cone-like illumination pattern of highly ionized gas which must be directly illuminated by the nucleus.
- The third image shows the radio jet.
- The last radio image shows a tiny structure which has the right size, orientation, and temperature to be the obscuring disk.

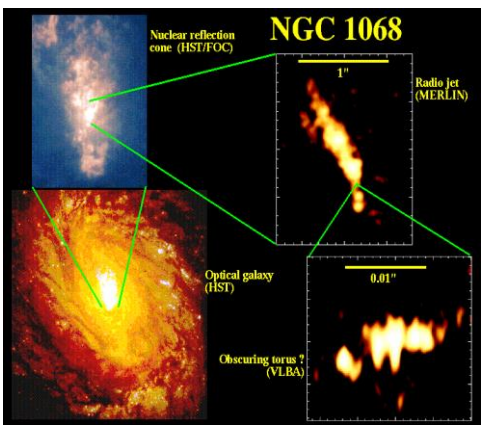

60

H-α line flux is proportional to the continuum flux at 480nm for a large range in luminosity.

Implies a common origin for both the narrow and the broad lines and supports the unified model.

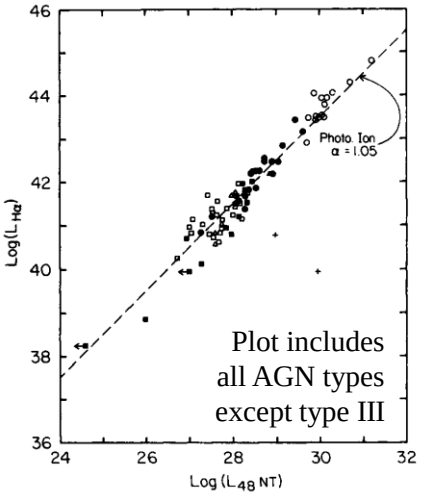

Figure 26.21 The luminosity in the H_α emission line versus the luminosity of the featureless continuum at a wavelength near 4800 Å (both in ergs s^{-1}). The symbols are QSOs (open circles), Seyfert 1s (filled circles), Seyfert 2s (open squares), NLRGs (triangles), and more Seyfert 2s and NLRGs (filled squares). (Figure from Shuder, *Ap. J.*, *244*, 12, 1981.)

61

QSO Evolution

- QSOs are some of the most distant objects in the universe.
- We want to know where QSOs came from, how they were formed, how they evolved, how long they live and what is ultimately likely to happen to them.
- We can use the observed properties of a large QSO population as a function of redshift (essentially the look-back time) to try to understand the evolution of individual AGN.

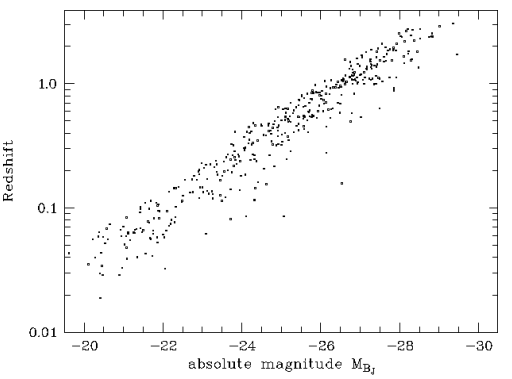

- The large luminosities of QSOs allow their detection to very large distances and therefore at times when the universe was very much younger than it is now.
- We will also learn about the formation of ordinary galaxies.
- The diagram here is based on a complete sample of QSOs and shows that the QSO population was brighter in the past.

62

- QSO luminosity functions for different look-back times show that QSO's were either brighter or more common (or both) in the past.
- About 1 in 10,000 galaxies hosts a QSO today (i.e. at z=0).
- At z~2 a typical QSO is about 16 times brighter than one at z=0 (horiz. line)
- QSO's as bright as the brightest ones in the local universe were ~300 times more common at z~2 (vert. line).

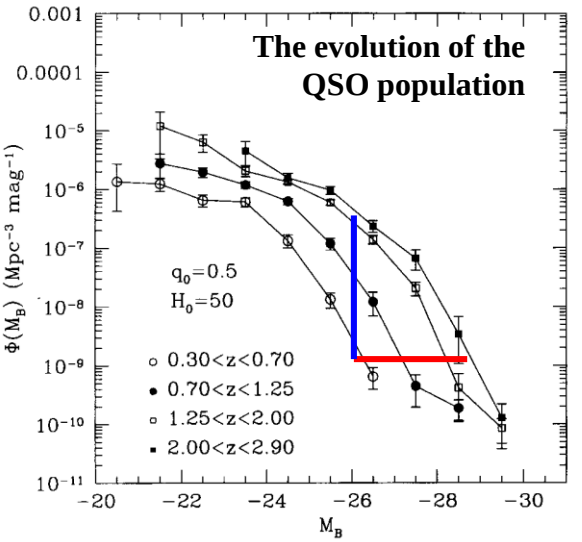

Figure 26.16 Luminosity functions for QSOs with different redshifts. (Figure from Boyle, B. J., *The Environment and Evolution of Galaxies*, Shull and Thronson (eds.), Kluwer Academic Publishers, Dordrecht, 1993.)

63

AGN evolution scenario – 1 - unlikely

- Only 1% - 3% of galaxies have a central massive black hole.
- The mass accretion rate on to the black hole was at its peak at $2 < z < 3$.
- The mass accretion rate on to the black hole has steadily declined as the universe has got older.
- Would therefore expect to see a few galaxies at z=0 with central black holes of 10^9 to 10^{10} solar masses.

AGN evolution scenario – 2 – likely

- All galaxies have a central massive black hole.
- The mass accretion rate on to the black hole is sporadic. AGN switches on and off. Maybe the activity is associated with galaxy-galaxy mergers.
- Bursts are about 10^8 years long.
- The number and strength of the bursts have decreased with time.
- In this scenario expect to see black hole masses in all local galaxies of ~10^6-10^8 solar masses.

64

QSO Evolution

- If only the number per unit volume changes we have pure **density evolution** (a vertical shift).
- If only the luminosity changes we have pure **luminosity evolution** (a horizontal shift).
- We could have a combination of both density and luminosity evolution.
- The work has been made more difficult because of the lack of data on faint objects at high redshifts.
- There is also a lack of bright objects at low redshifts because there simply isn't enough volume locally to find these very rare objects.

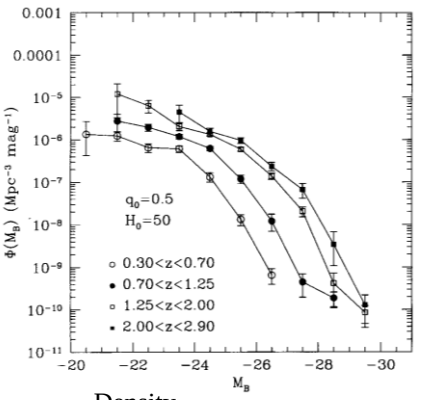

Density evolution

Luminosity evolution

65

QSO Evolution

- If we integrate the luminosity function down to an absolute magnitude M ~ -24 and plot the number of quasars per unit volume against the look-back time (a look-back time of 1.0 corresponds to 13.7 billion years which is the age of the universe), we see a dramatic increase in density until τ=0.9 (z = 4.6) followed by a drop for redshifts z > 4.6.
- What are QSO lifetimes likely to be?
- Consider the mass of a black hole accreting at the Eddington limit, $L_{edd} = 4\pi GMm_p c/\sigma_t$.
- We can convert the Eddington luminosity into a mass assuming an efficiency for turning the accreting mass into energy, and we find that the mass will double every ~ $4x10^7$ years.
- The growth of a black hole at the Eddington limit therefore would imply that redshift z = 0 QSOs will be considerably brighter than those at z = 2. This certainly disagrees with the observations.
- We could also consider growth of the black hole at a constant rate, say 1 $M_\odot$ per year. This would imply that long-lived quasars produce black holes with mass M ~ 10^{10} $M_\odot$.

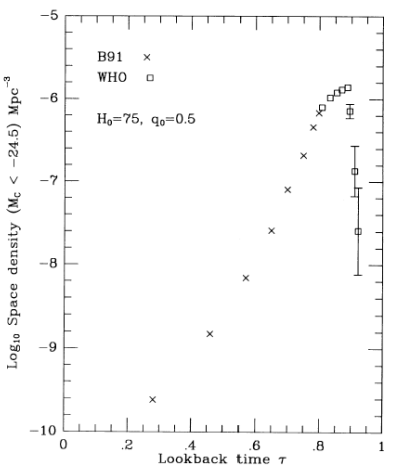

FIG. 8.—Space density of quasars with $M_c < -24.5(q_0 = 0.5)$ as a function of look-back time. The crosses show the results of the Boyle (1991) parameterization for quasars with $z \leq 1.9$. The open squares without error bars are derived from the values in Table 5 for the present sample for the double power-law model. Those with error bars come from the space density at $z = 3.3$ multiplied by the factor exp $[(3.3 - z)k_p]$ and for $k_p = 3.33^{+1.0}_{-1.0}$. The smooth joining of the Boyle points with the present results is an indication of the reliability of the present solution near $z \sim 2$. Note the decline in space density for $\tau > 0.9$.

66

M84 – evidence of a black hole

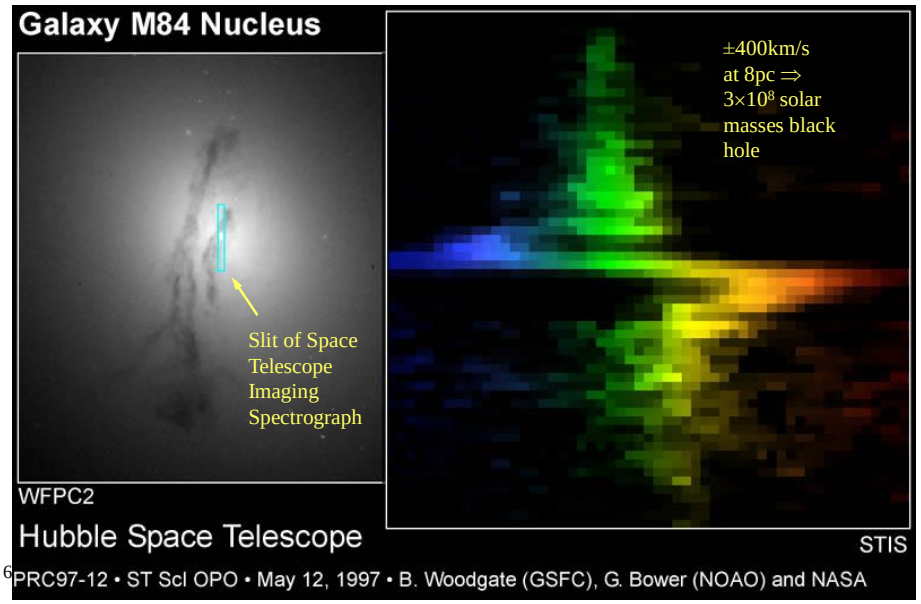

Black Holes in Nearby Galaxies

- The HST image (bottom left) and the spectrum (middle lower) of the core of the galaxy M87.
- The oxygen emission at 372.7 nm comes from excited gas and shows a systematic Doppler shift with position across the object.
- This is consistent with solid body rotation and a Keplerian fall-off at larger radii.
- The peak velocity is +/- 650 kms^{-1} at a radius of ~ 1 arcsec.

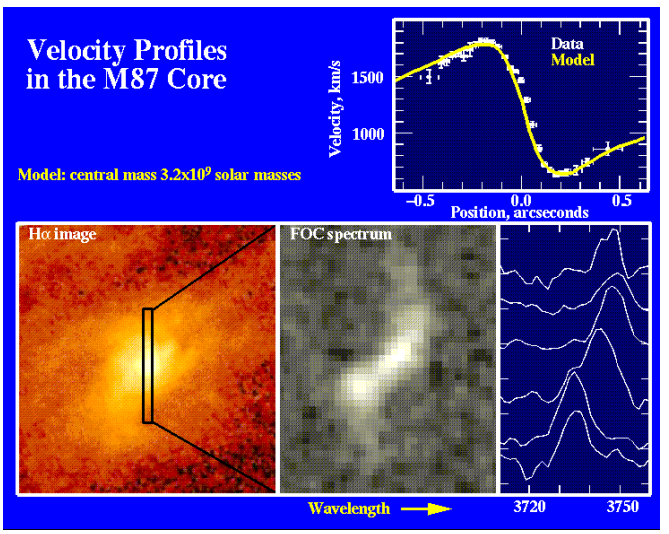

Velocity is known. Orbit size for the gas clouds is known because distance to the galaxy is known. This gives us the mass at the centre of the galaxy.

Black Holes in Nearby Galaxies: NGC4258

- With VLBI we can achieve an extremely high resolution, and determine the velocities close to the nucleus with high precision. The 22 GHz water maser line was used here.
- The galaxy NGC4258 is at a distance of 6.4 Mpc. The rotation curve shows that within 4.1 mas (= 0.13 pc) the total mass is $> 4 \times 10^9$ M.
- If this mass is in the form of a star cluster then the mean star separation would be ~ 100 AU, and the mean time between collisions would be $< 10^8$ years.
- The most natural explanation is a black hole with a mass $M = 3.6 \times 10^7 M_\odot$.

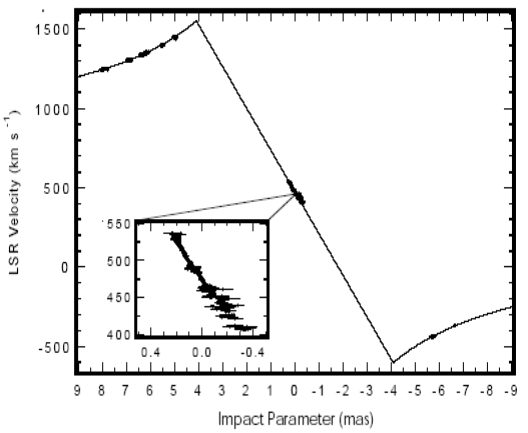

69

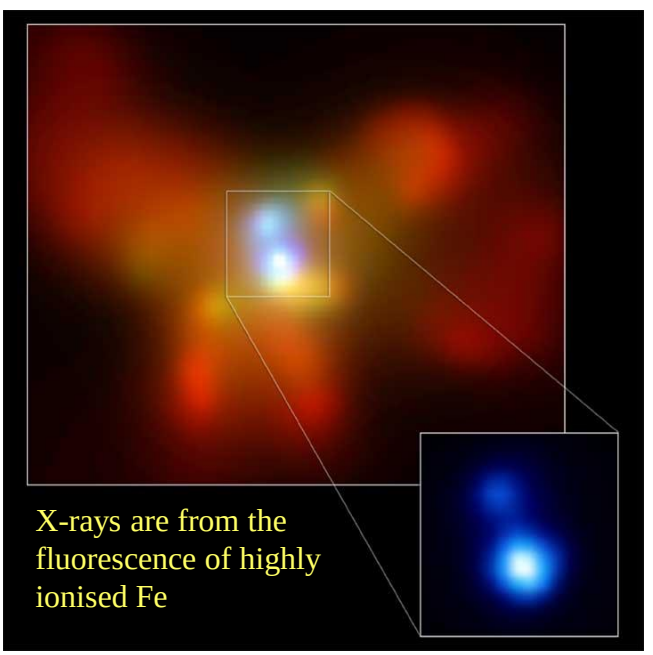

Double black hole at centre of NGC 6240

A galaxy-galaxy merger?

X-ray Chandra Image

70

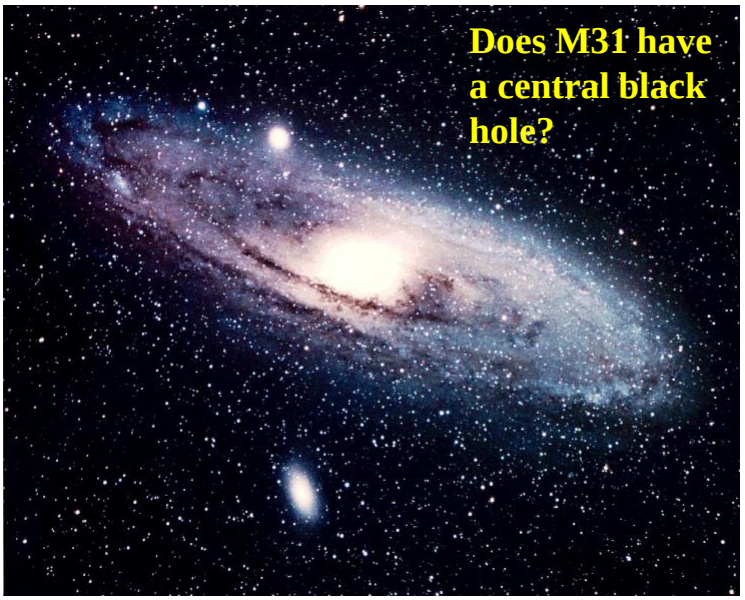

71

The black hole at the centre of M31

Virial mass from central velocity dispersion is ~7×10^7 solar masses.

From the rotation curve, within 4 pc there is a mass of ~2×10^7 solar masses.

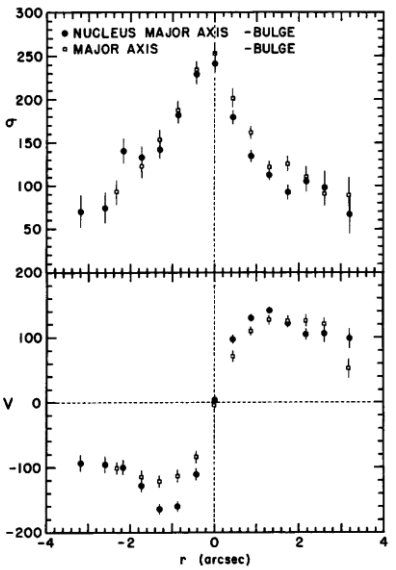

Figure 23.11 The stellar velocity dispersion and rotational velocities of stars near the center of M31, measured along the major axis of the bulge. Given the distance to Andromeda of 770 kpc, 2″ corresponds to a linear distance from the center of 7.5 pc. All velocities are in units of km s^{-1}. (Figure from Kormendy, *Ap. J.*, *325*, 128, 1988.)

72

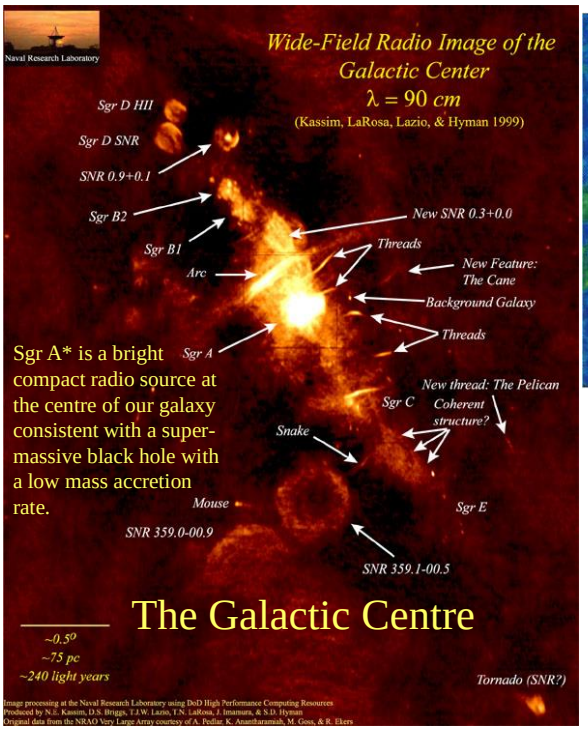
Naval Research Laboratory
Wide-Field Radio Image of the Galactic Center
λ = 90 cm
(Kassim, LaRosa, Lazio, & Hyman 1999)
Sgr D HII
Sgr D SNR
SNR 0.9+0.1
Sgr B2
Sgr B1
Arc
New SNR 0.3+0.0
Threads
New Feature: The Cane
Background Galaxy
Threads
Sgr A
Sgr A* is a bright compact radio source at the centre of our galaxy consistent with a super-massive black hole with a low mass accretion rate.
New thread: The Pelican
Sgr C
Coherent structure?
Snake
Mouse
Sgr E
SNR 359.0-00.9
SNR 359.1-00.5
The Galactic Centre
~0.5º
~75 pc
~240 light years
Tornado (SNR?)
Image processing at the Naval Research Laboratory using DoD High Performance Computing Resources
Produced by N.E. Kassim, D.S. Briggs, T.J.W. Lazio, T.N. LaRosa, J. Imamura, & S.D. Hyman
Original data from the NRAO Very Large Array courtesy of A. Pedlar, K. Anantharamaiah, M. Goss, & R. Ekers

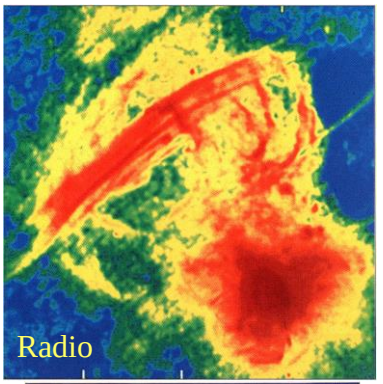
Radio

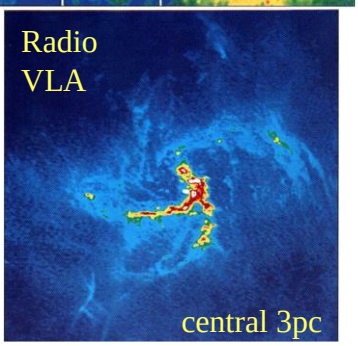
Radio
VLA
central 3pc

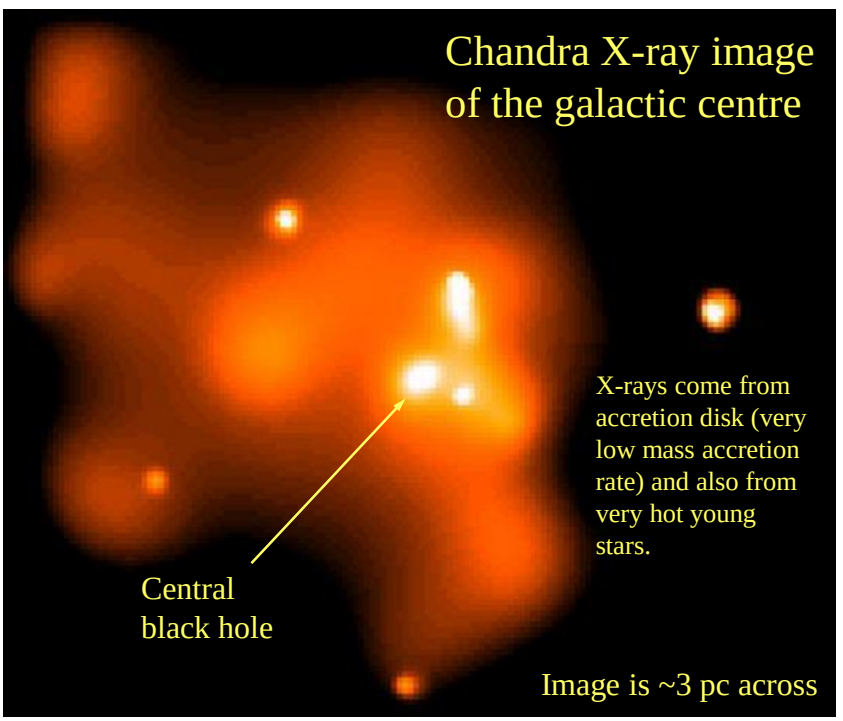
Chandra X-ray image of the galactic centre
X-rays come from accretion disk (very low mass accretion rate) and also from very hot young stars.
Central black hole
Image is ~3 pc across

74

Mass of the black hole at the galactic centre from stellar velocities (NIR observations)

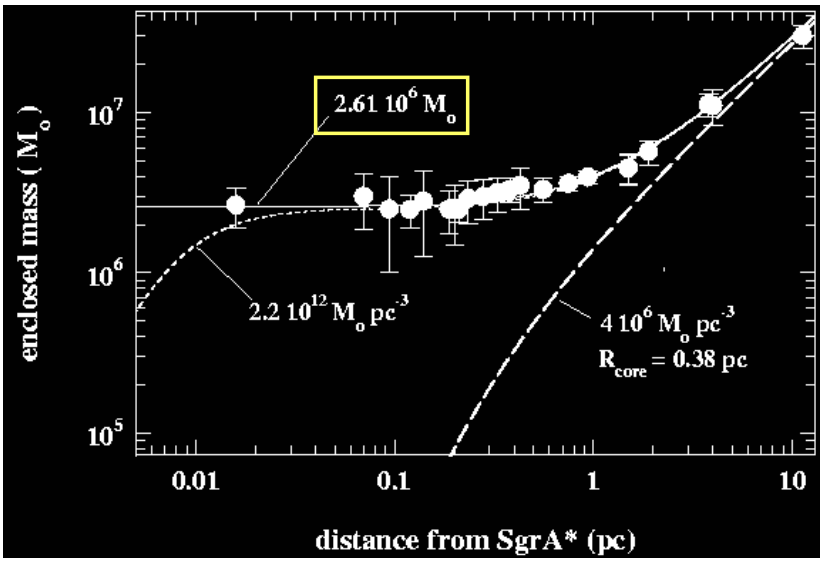

75

A BH at the centre of our Milky Way?

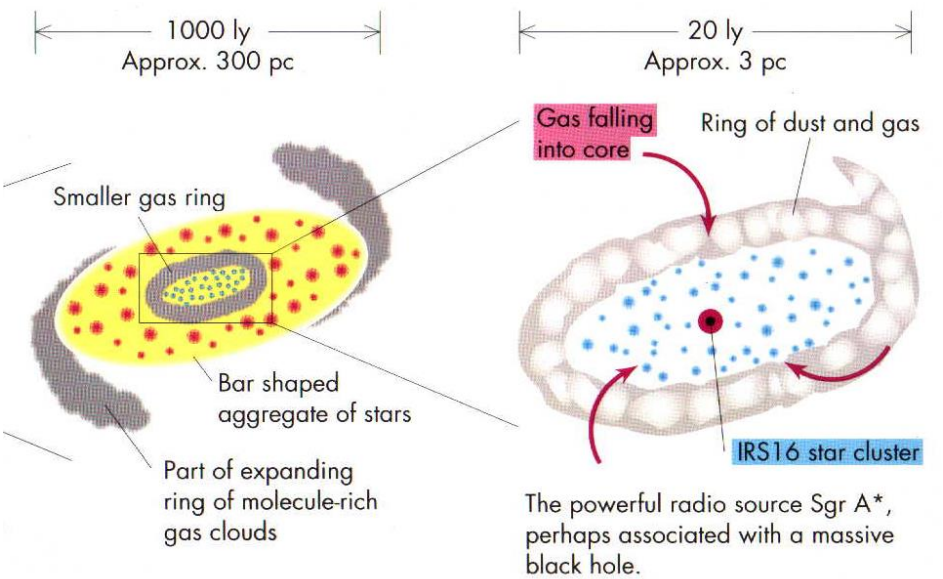

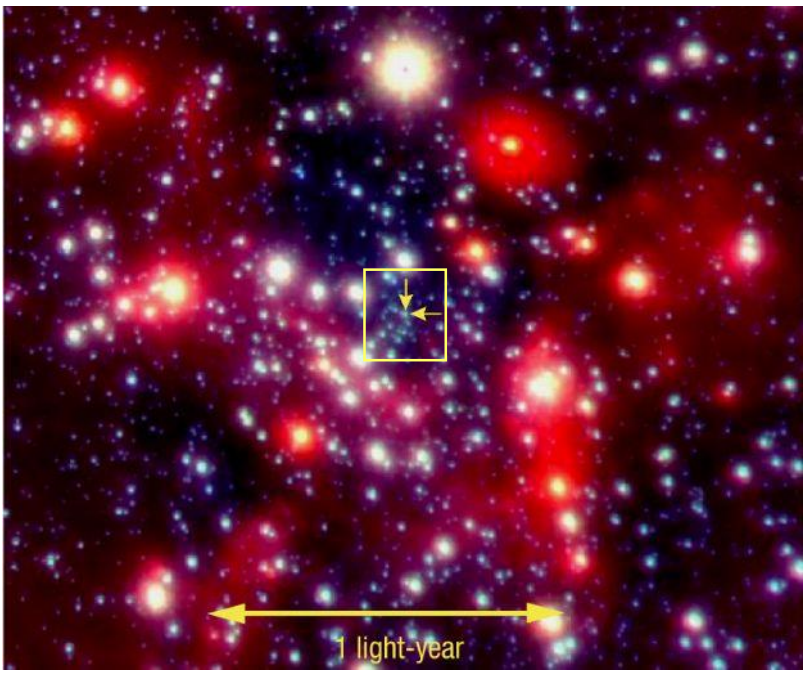

77

Star passes within
17 light-hours (~100AU)
of the centre.

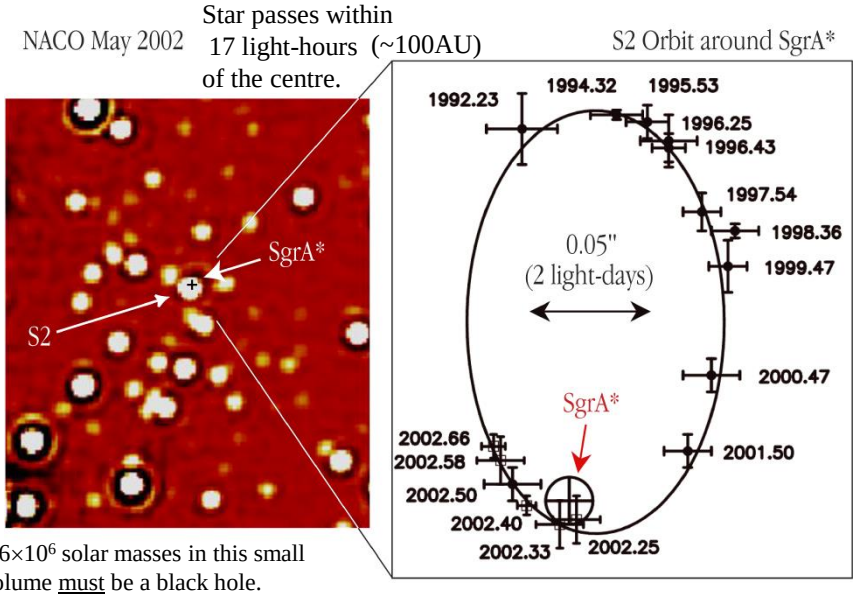

2.6×10^6 solar masses in this small volume must be a black hole.

78

The Motion of a Star around the Central Black Hole in the Milky Way

ESO PR Photo 23c/02 (9 October 2002)

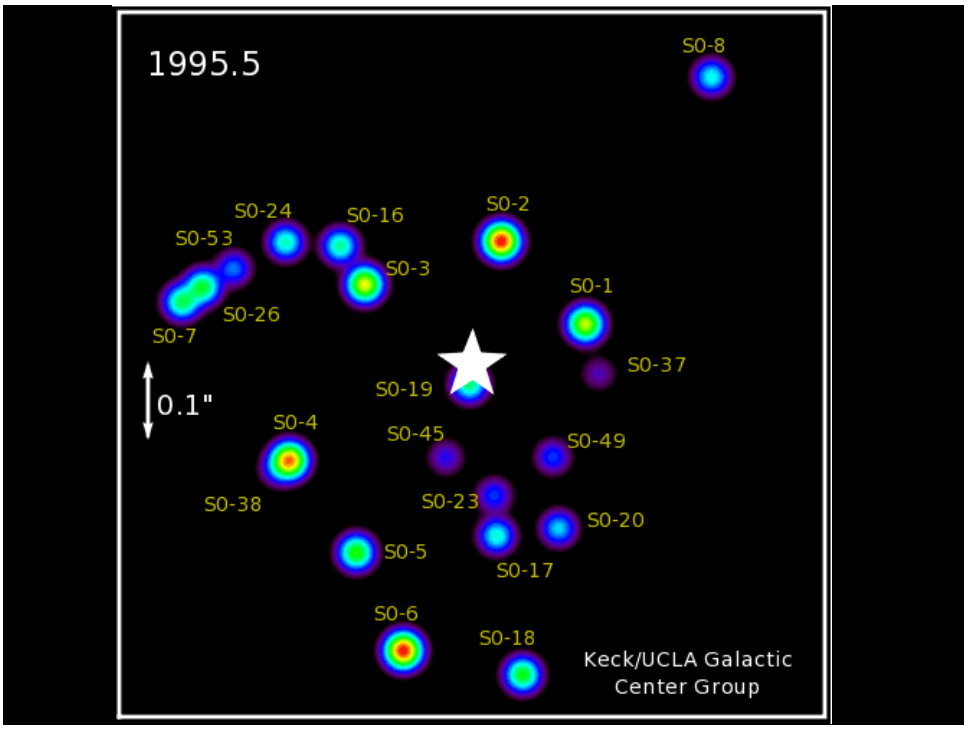
1995.5
S0-8
S0-24
S0-16
S0-2
S0-53
S0-3
S0-1
S0-26
S0-7
S0-37
0.1"
S0-19
S0-4
S0-45
S0-49
S0-38
S0-23
S0-20
S0-5
S0-17
S0-6
S0-18
Keck/UCLA Galactic
Center Group